Targeting acute myeloid leukemia by drug-induced c-MYB degradation

Vanessa Walf-Vorderwülbecke[1], Kerra Pearce[2], Tony Brooks[2], Mike Hubank[2], Marry M van den Heuvel-Eibrink[3,4], C Michel Zwaan[3], Stuart Adams[5], Darren Edwards[6], Jack Bartram[6], Sujith Samarasinghe[6], Philip Ancliff[6], Asim Khwaja[7], Nicholas Goulden[6], Gareth Williams[8,*], Jasper de Boer[1,*] and Owen Williams[1,*]

[1]Cancer Section, Developmental Biology and Cancer Programme, UCL Great Ormond Street Institute of Child Health, London, United Kingdom; [2]UCL Genomics, UCL Great Ormond Street Institute of Child Health, London, United Kingdom; [3]Department of Pediatric Oncology/Hematology, Erasmus-MC Sophia Children's Hospital, Rotterdam, Netherlands; [4]Princess Maxima Center for Pediatric Oncology, Utrecht, Netherlands; [5]SIHMDS-Haematology, Great Ormond Street Hospital for Children, London, United Kingdom; [6]Department of Paediatric Haematology, Great Ormond Street Hospital for Children, London, United Kingdom; [7]Department of Haematology, UCL Cancer Institute, London, UK; [8]Wolfson Centre for Age-Related Diseases, King's College London, London, UK.

Correspondence: Owen Williams or Jasper de Boer, Cancer Section, Developmental Biology and Cancer Programme, UCL GOSICH, 30 Guilford Street, London WC1N 1EH, UK. Phone: +44-207-9052180; E-mail: owen.williams@ucl.ac.uk or j.boer@ucl.ac.uk; Fax: +44-207-9052339.

[*]These authors contributed equally to this work.

Conflict of Interest statement: the authors have no conflict of interest to declare.

Running title: Mebendazole induced c-MYB degradation in AML

ABSTRACT

Despite advances in our understanding of the molecular basis for particular subtypes of acute myeloid leukemia (AML), effective therapy remains a challenge for many individuals suffering from this disease. A significant proportion of both pediatric and adult AML patients cannot be cured and since the upper limits of chemotherapy intensification have been reached, there is an urgent need for novel therapeutic approaches. The transcription factor c-MYB has been shown to play a central role in the development and progression of AML driven by several different oncogenes, including mixed lineage leukemia (*MLL*)-fusion genes. Here, we have used a *c-MYB* gene expression signature from *MLL*-rearranged AML to probe the Connectivity Map database and identified mebendazole as a c-MYB targeting drug. Mebendazole induces c-MYB degradation via the proteasome by interfering with the heat shock protein 70 (HSP70) chaperone system. Transient exposure to mebendazole is sufficient to inhibit colony formation by AML cells, but not normal cord blood-derived cells. Furthermore, mebendazole is effective at impairing AML progression *in vivo* in mouse xenotransplantation experiments. In context of the widespread human use of mebendazole, our data indicate that mebendazole induced c-MYB degradation represents a safe and novel therapeutic approach for AML.

INTRODUCTION

Rational combination of intensive chemotherapy with risk stratification has revolutionized the treatment of acute leukemia in children. However, progress has not been uniform across all subtypes of disease and many pediatric[1] and adult[2] Acute Myeloid Leukemia (AML) patients cannot be cured by current therapies. It is widely accepted that further intensification of chemotherapy is unlikely to improve outcomes,[3, 4] but that this may be achieved by developing novel therapeutics targeting specific leukemia drug-susceptibilities.

Rearrangements of the *MLL* gene are often associated with AML in children, and less frequently in adults.[5] These abnormalities result in generation of MLL fusion proteins, which are responsible for driving development of the disease. These proteins hijack the normal epigenetic machinery in developing hematopoietic cells, enforcing transcriptional dysregulation of target genes.[6-9] Identification of components of the MLL fusion-associated complexes led to a number of drug discovery initiatives.[10, 11] Recent studies indicate that one transcriptional target in particular, encoding the transcription factor c-MYB, is responsible for maintaining aberrant hematopoietic self-renewal programs necessary for initiation and progression of *MLL*-rearranged AML.[12-15]

c-MYB is highly expressed in immature hematopoietic progenitor cells and is required for definitive hematopoiesis,[16] normal myelopoiesis[17] and maintenance of adult hematopoietic stem cell (HSC) self-renewal.[18] *c-MYB* is rarely mutated in human leukemia, but has long been associated with hematopoietic malignancies.[19, 20] Some leukemia cells have been shown to be more sensitive to c-MYB inhibition than normal hematopoietic cells.[21, 22] This led to the hypothesis that although it may not be an oncogenic driver itself, certain cancers are nevertheless 'addicted' transcriptional dysregulation by c-MYB.[23] In contrast to absolute c-MYB deficiency, low levels of c-MYB expression are compatible with limited

hematopoiesis, especially myelopoiesis,[15, 24] suggesting that a window may exist for therapeutic targeting of c-MYB in AML. However, difficulties associated with developing small molecule inhibitors of transcription factor activity suggest that alternative approaches may be required to target c-MYB.[19] For example, the interaction between c-MYB and the transcriptional co-activator p300 was recently shown to be essential for AML induction[25] and to have promising potential as a target for pharmacological inhibition.[26]

In order to identify bioactive compounds capable of inhibiting c-MYB transcriptional activity in AML, we screened the Connectivity Map (CMAP) database with a c-MYB gene expression signature derived from integrating MLL-fusion protein specific gene expression changes with a list of previously published direct c-MYB target genes.[27, 28] This analysis identified the anti-helminth drug mebendazole as the top hit. We demonstrate that mebendazole induces proteasomal degradation of c-MYB, inhibits AML cell self-renewal and impairs AML progression *in vivo*. This work demonstrates that mebendazole has excellent potential for repurposing in novel AML therapies.

MATERIALS AND METHODS

Mice

Mice were maintained in the UCL GOSICH animal facilities and experiments were performed according to and approved by the United Kingdom Home Office regulations and followed UCL GOSICH institutional guidelines.

Human samples

For human AML samples (Supplementary Table 1), approval by the Institutional Review Board of the Erasmus MC for use of excess diagnostic material was obtained according to laws and regulations of the Netherlands, DB AML 01 (MEC-2010-370), AML NOPHO DBH 2012 (MEC-2014-024).

Global gene expression, SPIEDw and Gene set enrichment (GSEA) analyses

Analysis of MLL-ENL/MLL-AF9 gene expression changes (Geo repository: GSE59236) was performed using Affymetrix arrays (Affymetrix UK, High Wycombe, UK) and conditionally immortalized MLL-ENL and MLL-AF9 mouse myeloid cells.[29-32] Gene expression changes resulting from 6 hours exposure of THP1 cells to 10 μM mebendazole or DMSO were analysed by RNA-sequencing (Geo repository: GSE96544). A list (Supplementary Table 2) of human orthologs of MLL-ENL/MLL-AF9 gene expression changes, for genes also contained in the list of 1063 genes bound by c-MYB in mouse myeloid ERMYB cells[27] and deregulated in THP1 cells following siRNA-mediated c-MYB silencing,[28] were used to interrogate the CMAP database (https://portals.broadinstitute.org/cmap/)[33] using the SPIEDw web tool[34] (http://www.spied.org.uk/). For GSEA, c-MYB signatures were derived from Zhao et al.[27] and LSC signatures from Somervaille *et al*.[13]

Cell culture and reagents

Human AML cell lines were purchased from the ATCC (THP1) and DSMZ (OCI-AML3, NOMO-1, KCL22, U937, MV4;11, KASUMI-1 and SHI-1), authenticated by short tandem repeat profiling using the PowerPlex 16 system (Promega, Southampton, UK) and mycoplasma negative status confirmed using the MycoAlert Mycoplasma Detection Kit (Lonza, Verviers, Belgium). 293FT cells were from ThermoFisher Scientific (ThermoFisher Scientific, Hemel Hempstead, UK) and immortalized mouse myeloid cells were cultured as previously described.[29-32]

Colony formation assays

AML cell lines were plated in HSC002 (Bio Techne, Abingdon, UK), normal $CD34^+$ cord blood-derived cells (ZenBio, NC, USA) in HSC005 (Bio Techne) and primary AML cells in HSC005 methylcellulose medium supplemented with 50 ng/ml TPO and FLT3L.

Nematic protein organisation technique (NPOT) analysis

NPOT analysis was performed by INOVIEM Scientific (INOVIEM Scientific, Strasbourg, France).

In vivo transplantation

Luciferase expressing THP1 cells were transplanted into non-irradiated NOD-SCID-$\gamma^{-/-}$ (NSG; The Jackson Laboratory, Bar Harbor, ME, USA) mice. Recipient mice were imaged using the IVIS® Lumina Series III (PerkinElmer, Beaconsfield, UK) and randomly allocated to control or mebendazole-treated groups. Mebendazole (200 mg/kg of diet) was administered *ad libitum* in regular powdered diet, changed daily.

Lentivirus vector cloning

The ΔMYB cDNA[35] was cloned into the pCSGW-PIG vector, made by replacing the GFP cDNA from pCSGW[36] with a puro-IRES-GFP cassette. Lentiviral MISSION shRNA constructs targeting c-MYB (Clone ID:NM_005375.2-927s21c1), HSPA1A (sh1:Clone ID:NM_005345.4-1539s1c1; sh2:Clone ID:NM_005345.4-566s1c1) and the scramble (SCR) non-silencing control (SHC002) were purchased from Sigma-Aldrich (Gillingham, UK).

Western blot analysis

Antibodies against c-MYB (H-141, catalogue number sc-7874, Santa Cruz Biotechnology, Dallas, TX, USA; clone 1-1, catalogue number 05-175, Merck Millipore, Watford, UK; EPR718(2), catalogue number ab109127 , Abcam, Cambridge, UK), HSP70 (clone 242707, catalogue number MAB1663, Bio Techne), HSP70/HSC70 (and H-300, catalogue number sc-33575, and W27, catalogue number sc-24, Santa Cruz Biotechnology), Actin (I-19, catalogue number sc-1616, Santa Cruz Biotechnology), β-Actin (C4, catalogue number sc-47778, Santa Cruz Biotechnology), αTubulin (YL1/2, catalogue number sc-53029, Santa Cruz Biotechnology), SP1 (PEP 2, catalogue number sc-59, Santa Cruz Biotechnology) .

Microtubule depolymerization assay

Microtubule depolymerization was analysed as published previously.[37]

Quantitative RT-PCR analysis

Quantitative RT-PCR (qPCR) was performed on isolated mRNA using TaqMan probe based chemistry and an ABI Prism 7900HT fast Sequence Detection System (Life Technologies, Paisley, UK). All primer/probe sets were from Applied Biosystems, Life Technologies.

Statistics

Statistical significance was determined using Prism (GraphPad) software. Statistical analysis of survival curves was performed using the Mantel-Haenszel log-rank test. Statistical analysis of means was performed using the one sample *t* test or unpaired Student's *t* test, two-tailed *P* values < 0.05 being considered statistically significant. Variance was similar between groups.

Further details are provided in Supplementary Materials and Methods.

RESULTS

To identify candidate anti-leukemia drugs, we generated a therapeutic signature (Supplementary Table 2) by integrating gene expression changes due to MLL fusion silencing[29-32] with transcriptional regulation by c-MYB in acute myeloid leukemia.[27, 28] This signature was then used to interrogate drug-induced gene expression profiles in the CMAP database[33] using the SPIEDw web tool[34] (Figure 1a). The top hit resulting from this analysis was the anti-helminth agent mebendazole (Figure 1b).

In order to determine whether mebendazole was able to interfere with c-MYB regulated transcriptional pathways in human AML cells, RNASeq was performed on the MLL-AF9 expressing cell line THP1, following short-term exposure to the drug. GSEA of mebendazole induced gene expression changes confirmed that this drug was able to reverse both activation and repression by c-MYB of its target genes (Figure 1c and Supplementary Figure 1). Mebendazole exhibited anti-leukemia activity against *MLL* rearranged and non-rearranged human AML cell lines (Figure 2a and Supplementary Figure 2) and was effective at blocking their colony forming activity (Figure 2b and Supplementary Figure 3). This is not surprising, since c-MYB has also been shown to play a critical function in non-rearranged subtypes of AML.[25, 26, 38-41] Indeed, shRNA mediated silencing of c-MYB expression had a severe impact on colony formation (Supplementary Figure 4).

We then examined whether mebendazole interfered with c-MYB regulated gene expression by targeting the transcription factor directly, by examining RNA and protein expression 6 hours after exposure of AML cells to the drug. Interestingly, mebendazole inhibited c-MYB protein expression in all cell lines examined, and RNA expression in some (Figure 3a). c-MYB protein expression was affected at lower concentrations of mebendazole than those required to inhibit RNA expression, and occurred without any change in RNA

expression in some cells, suggesting that mebendazole targets c-MYB expression primarily at the protein level. Indeed, reversal of c-MYB protein loss by proteasomal inhibition indicates that mebendazole targets c-MYB for proteasomal degradation (Figure 3b and Supplementary Figure 5).

There has been considerable interest recently in repurposing mebendazole for cancer therapy.[42] However, the mechanism for its anti-cancer activity has remained elusive. Initially this was thought to derive from its microtubule destabilizing activity, mebendazole binding tubulin at the colchicine-site,[43] although recent experiments have suggested alternative mechanisms.[44] We compared microtubule depolymerization and c-MYB degradation induced by mebendazole in AML cells to that resulting from treatment of the cells with the microtubule disrupting agent colcemid (Figure 4a and Supplementary Figure 6). Equivalent concentrations of colcemid induced both microtubule depolymerization and loss of c-MYB protein. In contrast, mebendazole induced c-MYB degradation at concentrations that do not cause microtubule depolymerization, indicating that the former is not a result of the latter *per se*.

Exactly how mebendazole induces c-MYB degradation is unclear. It does not appear to be a secondary consequence of a cell cycle block, since c-MYB loss is already evident in THP1 cells after 4 hours mebendazole exposure, prior to drug-induced changes in cell cycle profiles (Supplementary Figure 7). In order to address this question, nematic protein organisation technique (NPOT) analysis (Inoviem Scientific) of mebendazole was performed using cell lysates from a primary AML patient sample and THP1 cells (Supplementary Figures 8a and 8b). DAVID analysis of the proteins identified in the AML patient sample hetero-assemblies, induced by mebendazole, highlighted ‘protein folding’ as the second most significant functional category, with 12 of the 16 proteins in this category also identified in THP1 hetero-assemblies (Supplementary Figure 8c). This suggests that mebendazole disrupts the

cellular protein folding machinery leading to the proteasomal targeting of c-MYB (Figure 3b). Of particular interest were a number of proteins of the HSP70/HSP90 chaperone complexes. c-MYB has previously been shown to be an HSC70 client protein in prostate cancer cells.[45, 46] Indeed, we found that the HSP70/HSC70 chaperone complex is also associated with c-MYB in AML cells (Figure 4b and Supplementary Figure 9a), an association that was lost upon exposure to mebendazole (Figure 4c). Furthermore, *HSPA1A* knockdown and pharmacological HSP70 inhibition resulted in reduced c-MYB protein levels (Figure 4d and Supplementary Figure 9b and 9c). However, mebendazole did not induce any changes in expression levels or subcellular re-localization of the HSP70/HSC70 complex (Supplementary Figure 9d).

Since c-MYB has been placed at the center of a leukemia stem cell (LSC) transcriptional self-renewal program in *MLL*-rearranged leukemia,[13] we hypothesized that mebendazole treatment of *MLL*-rearranged AML cells would inhibit this program. Indeed, GSEA analysis of gene expression changes following treatment of THP1 cells with mebendazole demonstrated negative enrichment of the LSC self-renewal signature (Figure 5a). In order to examine whether short-term exposure to mebendazole would indeed compromise AML cell self-renewal, we treated THP1 cells with 10μM mebendazole for 16 hours, washed them and examined their colony forming potential *in vitro*. Consistent with the observed inhibition of the LSC self-renewal program, transient exposure to mebendazole resulted in a more than 80% reduction in colony formation by THP1 cells (Figure 5b). Our hypothesis predicts that stabilization of the c-MYB protein would have the potential to rescue this loss of self-renewal induced by mebendazole. In order to examine this possibility, we generated a C-terminal deletion mutant of c-MYB (ΔMYB), previously shown to result in enhanced protein stability,[35] and expressed this mutant in THP1 cells. ΔMYB was partially protected from mebendazole-induced degradation (Figure 5c). Since the mutant contained the unaltered

DNA-binding domain, which is necessary for the transcriptional activity of c-MYB, but which contains residues known to be targeted by ubiquitin-mediated proteasomal degradation,[47] it is not surprising that it was not completely resistant to mebendazole. However, ΔMYB expressing THP1 cells were found to express higher levels of total c-MYB protein than control THP1 cells, following 6 hours treatment with mebendazole (Figure 5c). Importantly, this partial rescue of c-MYB protein expression correlated with increased colony forming potential of ΔMYB expressing THP1 cells following transient exposure to mebendazole (Figure 5d). These data indicate that mebendazole inhibits AML colony formation by disrupting the c-MYB regulated LSC self-renewal program. Interestingly, transient mebendazole exposure also inhibited *in vitro* colony formation by two independent MLL-AF9 expressing primary AML patient samples, but had no significant effect on colony formation by normal $CD34^+$ cord blood cells (Figure 5e and Supplementary Figure 10). Interestingly, mebendazole only caused partial loss of c-MYB in the latter (Supplementary Figure 11).

Having shown the anti-leukemia activity of mebendazole *in vitro*, we decided to test whether it could make an impact on AML disease progression *in vivo*. Oral administration of mebendazole, by simply mixing the drug in the diet, was found to have significant activity against disease in THP1 transplanted NSG mice, inhibiting leukemia progression (Figures 6a and b) and prolonging survival of treated mice (Figure 6c). Interestingly, THP-1 cells isolated from mebendazole-treated mice were found to express increased c-MYB protein levels and to be more resistant to drug treatment (Supplementary Figure 12). These data indicate that oral administration of mebendazole is sufficient to significantly impair AML progression *in vivo*.

DISCUSSION

Our data show that mebendazole induces degradation of the transcription factor c-MYB. c-MYB is essential for survival and self-renewal of multiple AML subtypes. c-MYB degradation results in loss of AML cell viability, colony formation and impaired *in vivo* leukemia progression. The rescue of AML cells from the inhibition of colony formation, following transient exposure to mebendazole, by over-expression of the ΔMYB mutant highlights the significance of c-MYB degradation in the anti-AML effects of this drug. Although, the ΔMYB mutant exhibits enhanced protein stability,[35] it is not completely resistant to mebendazole induced degradation, potentially explaining why the rescue of colony formation is only partial. It is likely that mebendazole interferes with multiple pathways in cancer cells[44] and it has been suggested to be a promising candidate for anti-cancer drug repurposing.[42] However, the induction of c-MYB degradation by mebendazole makes it particularly suitable to repurposing into AML therapy.

Some solid cancers are also addicted to continued and relatively high expression of the oncoprotein c-MYB. This is particularly evident in colorectal cancer where c-MYB is over-expressed and essential to continued proliferation and tumor cell survival.[19] In a recent study, mebendazole showed activity in the majority of the colon cancer cell lines tested.[44] It is noteworthy that a patient with refractory metastatic colon cancer treated with mebendazole showed near complete remission of the metastases in the lungs and lymph nodes and a good partial remission in the liver.[48] This suggests that mebendazole induced proteolysis of c-MYB may also have major clinical implications outside of AML therapy, in the treatment of a variety of cancers.

Induction of c-MYB degradation by mebendazole is blocked by proteasomal inhibition and occurs at much lower concentrations than those necessary to achieve microtubule

depolymerization in AML cells. We present evidence for the involvement of the HSP70/HSC70 chaperone complex in c-MYB targeting by mebendazole. The complex was found to bind c-MYB in AML cells, an association that was lost upon exposure of cells to mebendazole. Pharmacological or shRNA directed inhibition of HSP70 also resulted in loss of c-MYB protein. Interestingly, the HSP70/HSC70 complex has previously been shown to interact with c-MYB in prostate cancer cells, its displacement form the complex by glioma pathogenesis-related protein 1 (GLIPR1) over-expression resulting in c-MYB protein destabilization.[45, 46]

In summary, we have used Connectivity Map analysis to identify mebendazole as a novel candidate anti-AML therapeutic. Our data highlight a hitherto unappreciated link between microtubule interacting agents and the regulation of c-MYB protein degradation. Importantly, widespread use of mebendazole is tolerated in children and adults across the world,[49] suggesting that this drug has real potential for safe use in the treatment of human AML.

ACKNOWLEDGEMENTS

The authors thank Ayad Eddaoudi and Stephanie Canning, UCL GOSICH Flow Cytometry Facility, for providing assistance with flow cytometry, all staff of the UCL GOSICH Western Laboratories for excellent animal husbandry, and Didier Trono for lentiviral packaging constructs. JdB was supported by a fellowship from the Alternative Hair Charitable Foundation and GOSH Children's Charity (W1073), and VW-V (W1003) and OW (V1305, V2617) by grants from the GOSH Children's Charity.

REFERENCES

1 Pui CH, Carroll WL, Meshinchi S, Arceci RJ. Biology, risk stratification, and therapy of pediatric acute leukemias: an update. *J Clin Oncol* 2011; **29:** 551-565.

2 Bose P, Vachhani P, Cortes JE. Treatment of Relapsed/Refractory Acute Myeloid Leukemia. *Curr Treat Options Oncol* 2017; **18:** 17.

3 Tasian SK, Pollard JA, Aplenc R. Molecular therapeutic approaches for pediatric acute myeloid leukemia. *Front Oncol* 2014; **4:** 55.

4 Khan M, Mansoor AE, Kadia TM. Future prospects of therapeutic clinical trials in acute myeloid leukemia. *Future Oncol* 2017; **13:** 523-535.

5 Meyer C, Hofmann J, Burmeister T, Groger D, Park TS, Emerenciano M, *et al.* The MLL recombinome of acute leukemias in 2013. *Leukemia* 2013; **27:** 2165-2176.

6 Krivtsov AV, Armstrong SA. MLL translocations, histone modifications and leukaemia stem-cell development. *Nat Rev Cancer* 2007; **7:** 823-833.

7 Slany RK. The molecular biology of mixed lineage leukemia. *Haematologica* 2009; **94:** 984-993.

8 Somervaille TC, Cleary ML. Grist for the MLL: how do MLL oncogenic fusion proteins generate leukemia stem cells? *Int J Hematol* 2010; **91:** 735-741.

9 Muntean AG, Hess JL. The pathogenesis of mixed-lineage leukemia. *Annu Rev Pathol* 2012; **7:** 283-301.

10 Neff T, Armstrong SA. Recent progress toward epigenetic therapies: the example of mixed lineage leukemia. *Blood* 2013; **121:** 4847-4853.

11 Slany RK. The molecular mechanics of mixed lineage leukemia. *Oncogene* 2016; **35:** 5215-5223.

12 Hess JL, Bittner CB, Zeisig DT, Bach C, Fuchs U, Borkhardt A, *et al.* c-Myb is an essential downstream target for homeobox-mediated transformation of hematopoietic cells. *Blood* 2006; **108:** 297-304.

13 Somervaille TC, Matheny CJ, Spencer GJ, Iwasaki M, Rinn JL, Witten DM, *et al.* Hierarchical maintenance of MLL myeloid leukemia stem cells employs a transcriptional program shared with embryonic rather than adult stem cells. *Cell Stem Cell* 2009; **4:** 129-140.

14 Jin S, Zhao H, Yi Y, Nakata Y, Kalota A, Gewirtz AM. c-Myb binds MLL through menin in human leukemia cells and is an important driver of MLL-associated leukemogenesis. *J Clin Invest* 2010; **120:** 593-606.

15 Zuber J, Rappaport AR, Luo W, Wang E, Chen C, Vaseva AV, *et al.* An integrated approach to dissecting oncogene addiction implicates a Myb-coordinated self-renewal program as essential for leukemia maintenance. *Genes Dev* 2011; **25:** 1628-1640.

16 Mucenski ML, McLain K, Kier AB, Swerdlow SH, Schreiner CM, Miller TA, *et al.* A functional c-myb gene is required for normal murine fetal hepatic hematopoiesis. *Cell* 1991; **65:** 677-689.

17 Sumner R, Crawford A, Mucenski M, Frampton J. Initiation of adult myelopoiesis can occur in the absence of c-Myb whereas subsequent development is strictly dependent on the transcription factor. *Oncogene* 2000; **19:** 3335-3342.

18 Lieu YK, Reddy EP. Conditional c-myb knockout in adult hematopoietic stem cells leads to loss of self-renewal due to impaired proliferation and accelerated differentiation. *Proc Natl Acad Sci U S A* 2009; **106:** 21689-21694.

19 Ramsay RG, Gonda TJ. MYB function in normal and cancer cells. *Nat Rev Cancer* 2008; **8:** 523-534.

20 Pattabiraman DR, Gonda TJ. Role and potential for therapeutic targeting of MYB in leukemia. *Leukemia* 2013; **27:** 269-277.

21 Anfossi G, Gewirtz AM, Calabretta B. An oligomer complementary to c-myb-encoded mRNA inhibits proliferation of human myeloid leukemia cell lines. *Proc Natl Acad Sci U S A* 1989; **86:** 3379-3383.

22 Calabretta B, Sims RB, Valtieri M, Caracciolo D, Szczylik C, Venturelli D*, et al.* Normal and leukemic hematopoietic cells manifest differential sensitivity to inhibitory effects of c-myb antisense oligodeoxynucleotides: an in vitro study relevant to bone marrow purging. *Proc Natl Acad Sci U S A* 1991; **88:** 2351-2355.

23 Gonda TJ, Ramsay RG. Directly targeting transcriptional dysregulation in cancer. *Nat Rev Cancer* 2015; **15:** 686-694.

24 Emambokus N, Vegiopoulos A, Harman B, Jenkinson E, Anderson G, Frampton J. Progression through key stages of haemopoiesis is dependent on distinct threshold levels of c-Myb. *EMBO J* 2003; **22:** 4478-4488.

25 Pattabiraman DR, McGirr C, Shakhbazov K, Barbier V, Krishnan K, Mukhopadhyay P, *et al.* Interaction of c-Myb with p300 is required for the induction of acute myeloid leukemia (AML) by human AML oncogenes. *Blood* 2014; **123:** 2682-2690.

26 Uttarkar S, Dasse E, Coulibaly A, Steinmann S, Jakobs A, Schomburg C, *et al.* Targeting acute myeloid leukemia with a small molecule inhibitor of the Myb/p300 interaction. *Blood* 2016; **127:** 1173-1182.

27 Zhao L, Glazov EA, Pattabiraman DR, Al-Owaidi F, Zhang P, Brown MA, *et al.* Integrated genome-wide chromatin occupancy and expression analyses identify key myeloid pro-differentiation transcription factors repressed by Myb. *Nucleic Acids Res* 2011; **39:** 4664-4679.

28 Suzuki H, Forrest AR, van Nimwegen E, Daub CO, Balwierz PJ, Irvine KM, *et al.* The transcriptional network that controls growth arrest and differentiation in a human myeloid leukemia cell line. *Nat Genet* 2009; **41:** 553-562.

29 Horton SJ, Grier DG, McGonigle GJ, Thompson A, Morrow M, De Silva I, *et al.* Continuous MLL-ENL expression is necessary to establish a "Hox Code" and maintain immortalization of hematopoietic progenitor cells. *Cancer Res* 2005; **65:** 9245-9252.

30 Horton SJ, Walf-Vorderwulbecke V, Chatters SJ, Sebire NJ, de Boer J, Williams O. Acute myeloid leukemia induced by MLL-ENL is cured by oncogene ablation despite acquisition of complex genetic abnormalities. *Blood* 2009; **113:** 4922-4929.

31 Walf-Vorderwulbecke V, de Boer J, Horton SJ, van Amerongen R, Proost N, Berns A, *et al.* Frat2 mediates the oncogenic activation of Rac by MLL fusions. *Blood* 2012; **120:** 4819-4828.

32 Osaki H, Walf-Vorderwulbecke V, Mangolini M, Zhao L, Horton SJ, Morrone G, *et al.* The AAA+ ATPase RUVBL2 is a critical mediator of MLL-AF9 oncogenesis. *Leukemia* 2013; **27:** 1461-1468.

33 Lamb J, Crawford ED, Peck D, Modell JW, Blat IC, Wrobel MJ, *et al.* The Connectivity Map: using gene-expression signatures to connect small molecules, genes, and disease. *Science* 2006; **313:** 1929-1935.

34 Williams G. SPIEDw: a searchable platform-independent expression database web tool. *BMC Genomics* 2013; **14:** 765.

35 Corradini F, Cesi V, Bartella V, Pani E, Bussolari R, Candini O, *et al.* Enhanced proliferative potential of hematopoietic cells expressing degradation-resistant c-Myb mutants. *J Biol Chem* 2005; **280:** 30254-30262.

36 Demaison C, Parsley K, Brouns G, Scherr M, Battmer K, Kinnon C, *et al.* High-level transduction and gene expression in hematopoietic repopulating cells using a human immunodeficiency [correction of imunodeficiency] virus type 1-based lentiviral vector containing an internal spleen focus forming virus promoter. *Hum Gene Ther* 2002; **13:** 803-813.

37 Minotti AM, Barlow SB, Cabral F. Resistance to antimitotic drugs in Chinese hamster ovary cells correlates with changes in the level of polymerized tubulin. *J Biol Chem* 1991; **266:** 3987-3994.

38 Lidonnici MR, Corradini F, Waldron T, Bender TP, Calabretta B. Requirement of c-Myb for p210(BCR/ABL)-dependent transformation of hematopoietic progenitors and leukemogenesis. *Blood* 2008; **111:** 4771-4779.

39 Soliera AR, Lidonnici MR, Ferrari-Amorotti G, Prisco M, Zhang Y, Martinez RV, *et al.* Transcriptional repression of c-Myb and GATA-2 is involved in the biologic effects of C/EBPalpha in p210BCR/ABL-expressing cells. *Blood* 2008; **112:** 1942-1950.

40 Manzotti G, Mariani SA, Corradini F, Bussolari R, Cesi V, Vergalli J, *et al.* Expression of p89(c-Mybex9b), an alternatively spliced form of c-Myb, is required for proliferation and survival of p210BCR/ABL-expressing cells. *Blood Cancer J* 2012; **2:** e71.

41 Waldron T, De Dominici M, Soliera AR, Audia A, Iacobucci I, Lonetti A, *et al.* c-Myb and its target Bmi1 are required for p190BCR/ABL leukemogenesis in mouse and human cells. *Leukemia* 2012; **26:** 644-653.

42 Pantziarka P, Bouche G, Meheus L, Sukhatme V, Sukhatme VP. Repurposing Drugs in Oncology (ReDO)-mebendazole as an anti-cancer agent. *Ecancermedicalscience* 2014; **8:** 443.

43 Laclette JP, Guerra G, Zetina C. Inhibition of tubulin polymerization by mebendazole. *Biochem Biophys Res Commun* 1980; **92:** 417-423.

44 Nygren P, Fryknas M, Agerup B, Larsson R. Repositioning of the anthelmintic drug mebendazole for the treatment for colon cancer. *J Cancer Res Clin Oncol* 2013; **139:** 2133-2140.

45 Li L, Yang G, Ren C, Tanimoto R, Hirayama T, Wang J, *et al.* Glioma pathogenesis-related protein 1 induces prostate cancer cell death through Hsc70-mediated suppression of AURKA and TPX2. *Mol Oncol* 2013; **7:** 484-496.

46 Liu W, Vielhauer GA, Holzbeierlein JM, Zhao H, Ghosh S, Brown D, *et al.* KU675, a Concomitant Heat-Shock Protein Inhibitor of Hsp90 and Hsc70 that Manifests Isoform Selectivity for Hsp90alpha in Prostate Cancer Cells. *Mol Pharmacol* 2015; **88:** 121-130.

438 47 Tanikawa J, Ichikawa-Iwata E, Kanei-Ishii C, Nakai A, Matsuzawa S, Reed JC, *et al.*
439 p53 suppresses the c-Myb-induced activation of heat shock transcription factor 3. *J*
440 *Biol Chem* 2000; **275:** 15578-15585.

441 48 Nygren P, Larsson R. Drug repositioning from bench to bedside: tumour remission by
442 the antihelmintic drug mebendazole in refractory metastatic colon cancer. *Acta Oncol*
443 2014; **53:** 427-428.

444 49 Levecke B, Montresor A, Albonico M, Ame SM, Behnke JM, Bethony JM, *et al.*
445 Assessment of anthelmintic efficacy of mebendazole in school children in six
446 countries where soil-transmitted helminths are endemic. *PLoS Negl Trop Dis* 2014; **8:**
447 e3204.

448

FIGURE LEGENDS

Figure 1. Identification of mebendazole as a c-MYB targeting drug in AML. (**a**) Diagram summarizing the generation of a c-MYB signature used to interrogate the CMAP database [33] using SPIEDw[34]. (**b**) The 1,309 CMAP drugs are ranked based on the significance of regression scores between their transcriptional profiles and that of the query. The Z-score corresponds to the number of standard deviations of the score away from the mean. Inset is the structure of mebendazole (rank 1). (**c**) GSEA of the c-MYB activated (top) and repressed (bottom) gene sets in global gene expression changes in THP1 cells following 6 hours exposure to 10 μM mebendazole (MBZ) versus DMSO.

Figure 2. Mebendazole inhibits AML growth and colony formation. (**a**) Viability, normalized to DMSO controls, of AML cell lines treated for 72 hours with indicated mebendazole concentrations. Bars and error bars are means and SD of three independent experiments, each in triplicate. (**b**) Examples of AML cell line colony formation in methylcellulose cultures in the presence of DMSO or 1.25 μM mebendazole (quantification in Supplementary Figure 1).

Figure 3. Mebendazole induces proteasomal degradation of c-MYB. (**a**) Protein and RNA expression in AML cells after 6 hours treatment with DMSO or indicated mebendazole concentrations, normalized to DMSO controls. Bars and error bars are means and SD of three independent experiments. $*P < 0.05$; $**P < 0.01$; $***P < 0.001$; n.s. not significant (relative to DMSO controls), one sample *t* test. Western blots below graphs show examples of c-MYB protein expression. (**b**) Western blot analysis of c-MYB protein expression in AML cells after 6 hours treatment with DMSO, 10 μM mebendazole or 10 μM mebendazole and 10 μM MG132 (quantification in Supplementary Figure 3).

Figure 4. Mebendazole destabilizes c-MYB protein by interfering with the HSP70/HSC70 chaperone pathway. (**a**) Percent polymerized tubulin in THP1 cells following 6 hours

treatment with indicated concentrations of mebendazole (top left) or colcemid (top right), and western blot analysis of corresponding c-MYB protein expression (bottom). Tubulin stabilization by 5 μM paclitaxel (Pax) is also shown. Bars and error bars are means and SD of three independent experiments. *P < 0.05; **P < 0.01; ***P < 0.001; n.s. not significant, unpaired Student's t-test. (**b**) Western blot analysis of mouse IgG and anti-HSP70/HSC70 immunoprecipitates from THP1 cells, stained with anti-c-MYB (top) and anti-HSP70/HSC70 (bottom). Representative data from one of three independent experiments. (**c**) Western blot analysis of anti-HSP70/HSC70 immunoprecipitates from THP1 cells following 6 hours treatment with DMSO or 10 μM mebendazole, stained with anti-c-MYB (top) and anti-HSP70/HSC70 (bottom). Representative data from one of three independent experiments. (**d**) Western blot analysis of HSP70 (top) and c-MYB (middle) expression in THP1 cells 7 days after transduction with control scramble (shSCR) shRNA or two independent shRNA targeting *HSPA1A* (sh1 and sh2) (quantification in Supplementary Figure 7b).

Figure 5. Transient exposure to mebendazole inhibits colony formation by AML but not normal cord blood-derived hematopoietic cells. (**a**) GSEA of the gene expression signatures positively (top) and negatively (bottom) correlating with leukemia stem cell frequency [13] in global gene expression changes in THP1 cells following 6 hours exposure to 10 μM mebendazole versus DMSO. (**b**) Example of THP1 colony formation after pre-treatment with DMSO or 10 μM mebendazole. Cells were treated with vehicle or drug for 16 hours, washed and placed into methylcellulose culture. The mean (± SD) fold change in colony formation is shown from five independent experiments, normalized to DMSO controls. ***P < 0.001 (relative to DMSO controls), one sample *t* test. (**c**) c-MYB protein expression in empty vector (Con) or c-MYB deletion mutant (ΔMYB) transduced THP1 cells, 6 hours after treatment with DMSO or 10 μM mebendazole. (**d**) Fold change in colony formation by Con or ΔMYB transduced THP1 cells, following 16 hours pre-treatment with DMSO or 10 μM

mebendazole, normalized to Con or ΔMYB DMSO controls. Bars and error bars are means and SD of seven independent experiments. ***$P < 0.001$, unpaired Student's t-test. (**e**) Colony formation frequency by two independent primary AML patient samples (AML1547, AML1497) and two independent normal $CD34^+$ cord blood samples (CB1, CB2) after pre-treatment with DMSO or 10 μM mebendazole. Cells were treated with vehicle or drug for 20 hours, washed and placed into methylcellulose culture.

Figure 6. Mebendazole impairs AML progression *in vivo*. (**a**) Bioluminescence imaging of NSG recipient mice 10 days after injection with THP1-LUC2 cells, and before drug treatment, (day 0, top), and 22 days after treatment with normal or mebendazole-containing diet (bottom). Bars for luminescence signal represent photons/s/cm^2/steradian. (**b**) Luminescence signal in treatment groups, 10 days after THP1-LUC2 cell injection and before drug treatment (left), and fold increase in luminescence signal in the groups 7 and 17 days after treatment with normal or mebendazole-containing diet (right). Bars and error bars are means and SD of values form control (n = 5) and mebendazole-treated (n = 9) groups. ***$P < 0.001$; n.s. not significant, unpaired Student's t-test. (**c**) Survival curve for control (n = 9) and mebendazole-treated (n = 12) mice, $P < 0.0001$, Mantel-Haenszel log-rank test.

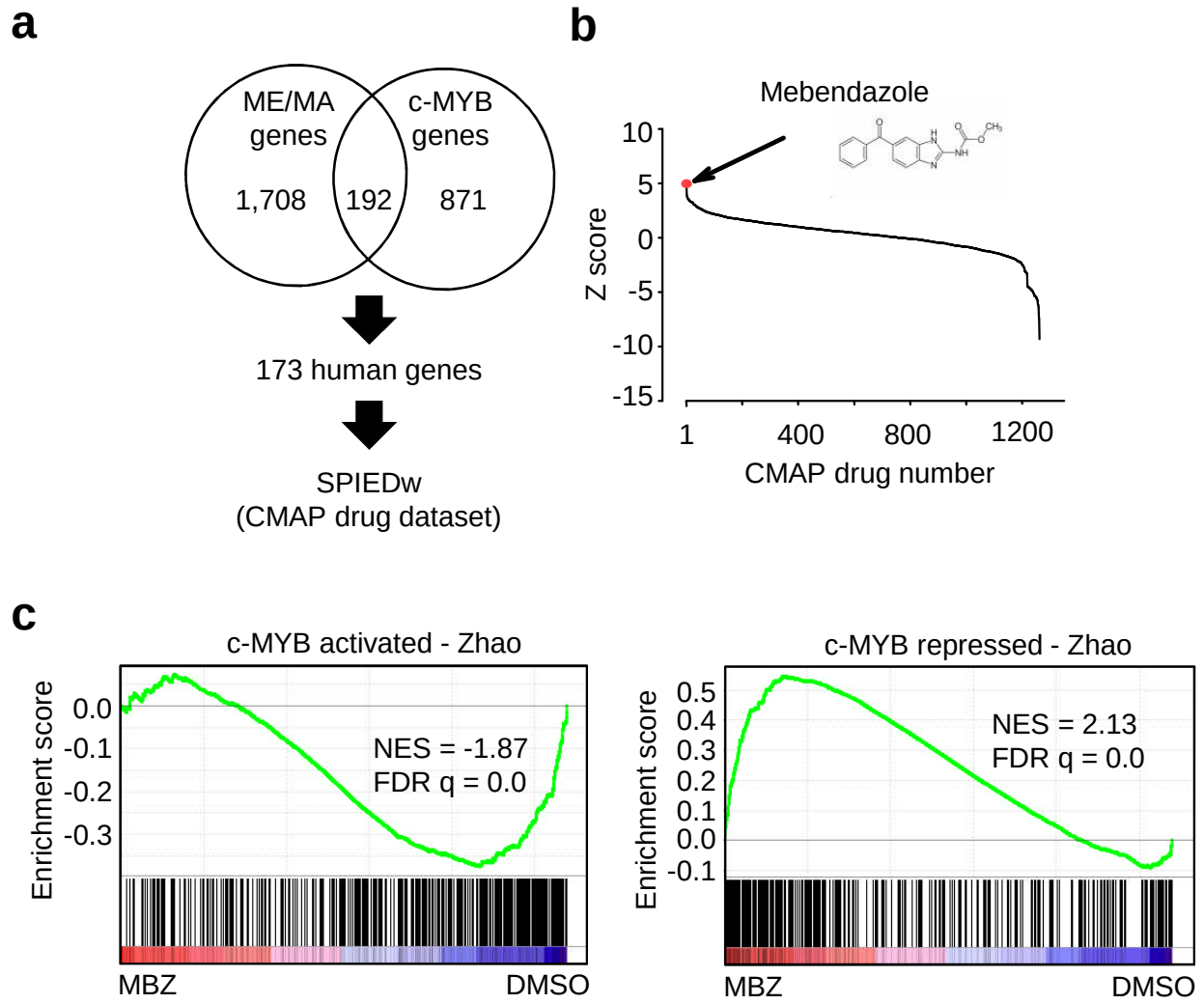
a
ME/MA genes
c-MYB genes
1,708
192
871
173 human genes
SPIEDw
(CMAP drug dataset)
b
Mebendazole
Z score
10
5
0
-5
-10
-15
1
400
800
1200
CMAP drug number
c
c-MYB activated - Zhao
Enrichment score
0.0
-0.1
-0.2
-0.3
NES = -1.87
FDR q = 0.0
MBZ
DMSO
c-MYB repressed - Zhao
Enrichment score
0.5
0.4
0.3
0.2
0.1
0.0
-0.1
NES = 2.13
FDR q = 0.0
MBZ
DMSO

FIGURE 1

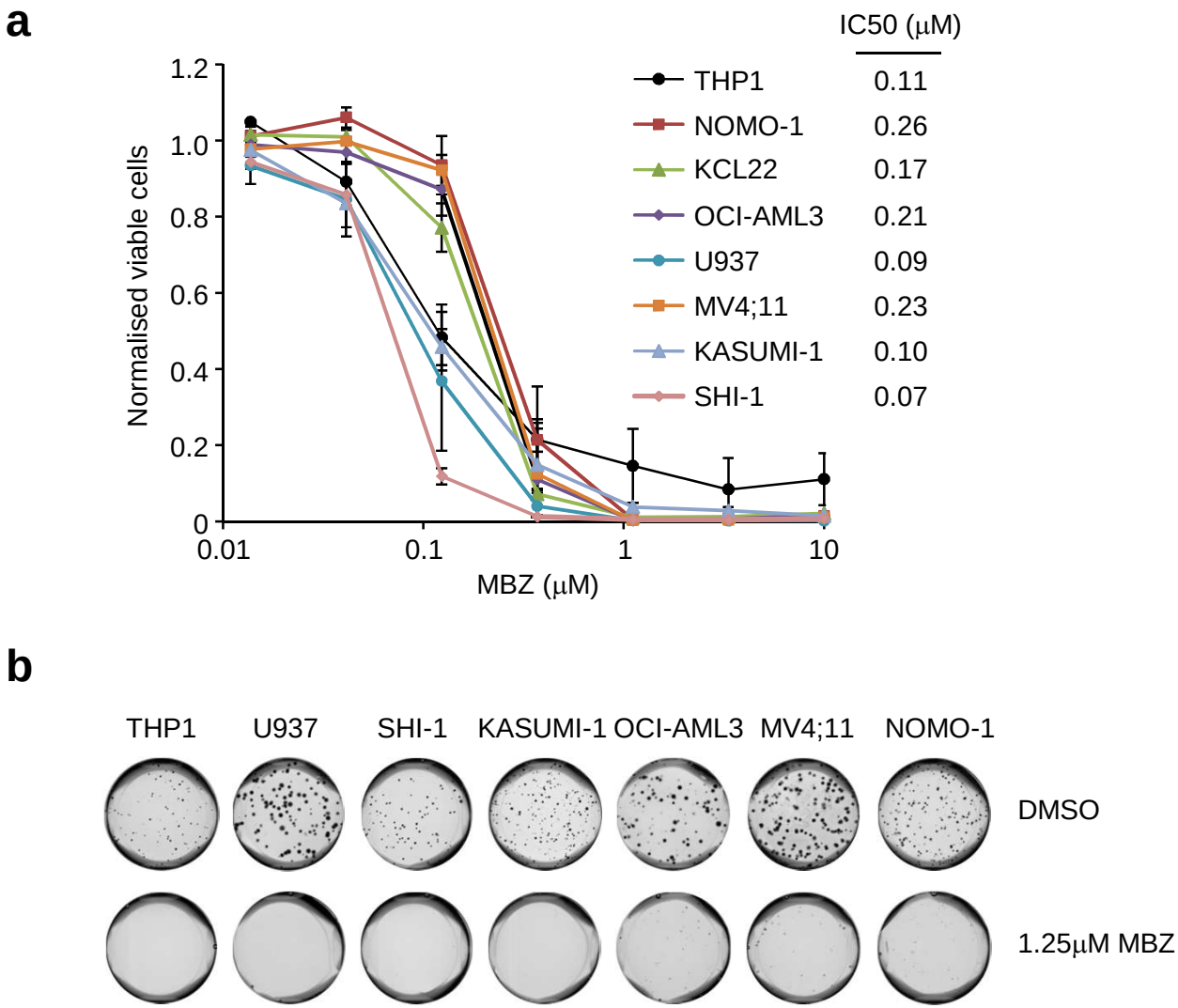
a
IC50 (μM)
THP1 0.11
NOMO-1 0.26
KCL22 0.17
OCI-AML3 0.21
U937 0.09
MV4;11 0.23
KASUMI-1 0.10
SHI-1 0.07
Normalised viable cells
1.2
1.0
0.8
0.6
0.4
0.2
0
0.01
0.1
1
10
MBZ (μM)
b
THP1
U937
SHI-1
KASUMI-1
OCI-AML3
MV4;11
NOMO-1
DMSO
1.25μM MBZ

FIGURE 2

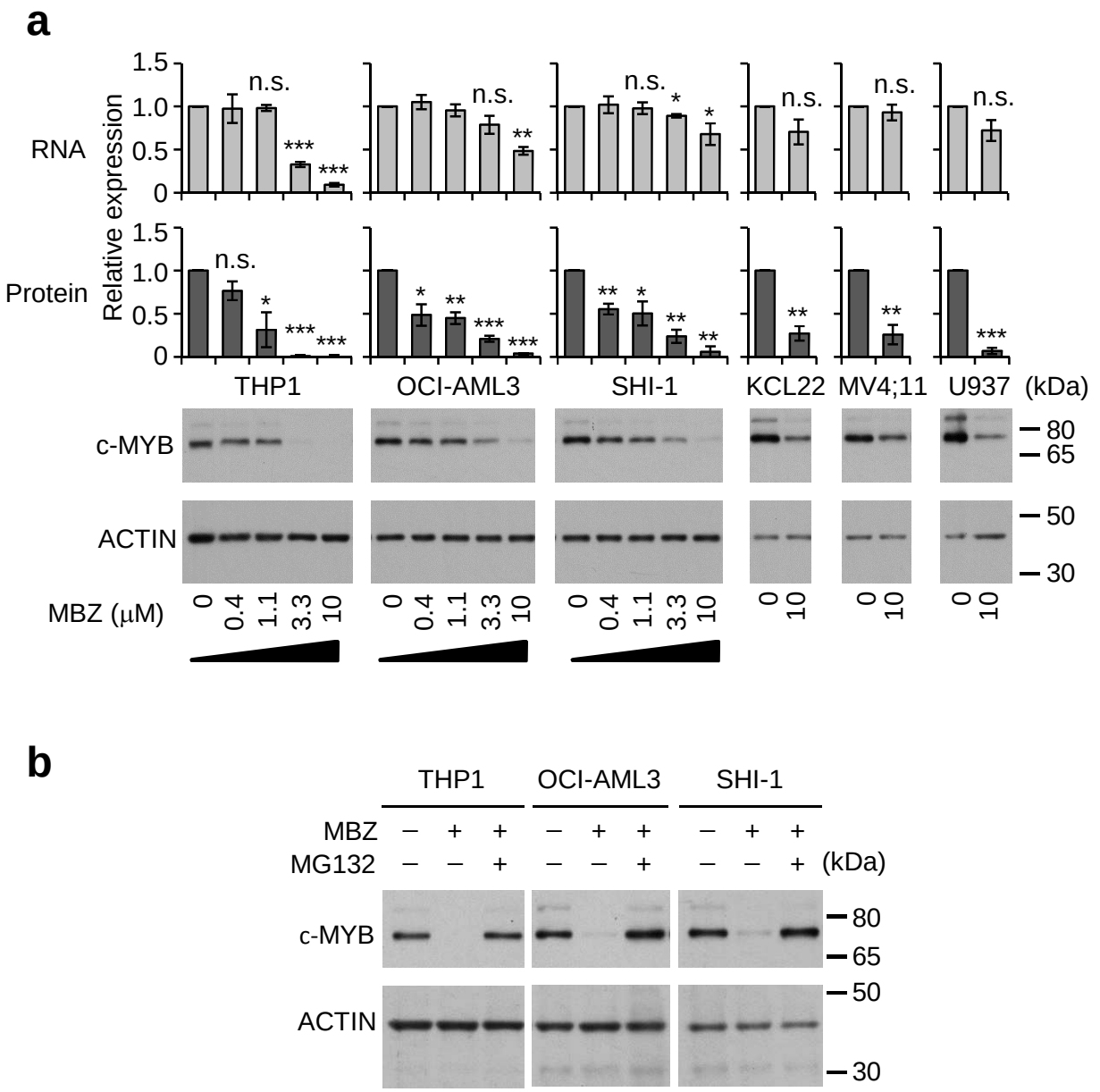
a
RNA
Protein
Relative expression
1.5
1.0
0.5
0
n.s.
*
**
***
THP1
OCI-AML3
SHI-1
KCL22
MV4;11
U937
(kDa)
c-MYB
ACTIN
80
65
50
30
MBZ (μM)
0
0.4
1.1
3.3
10
b
MBZ
MG132
–
+
(kDa)

FIGURE 3

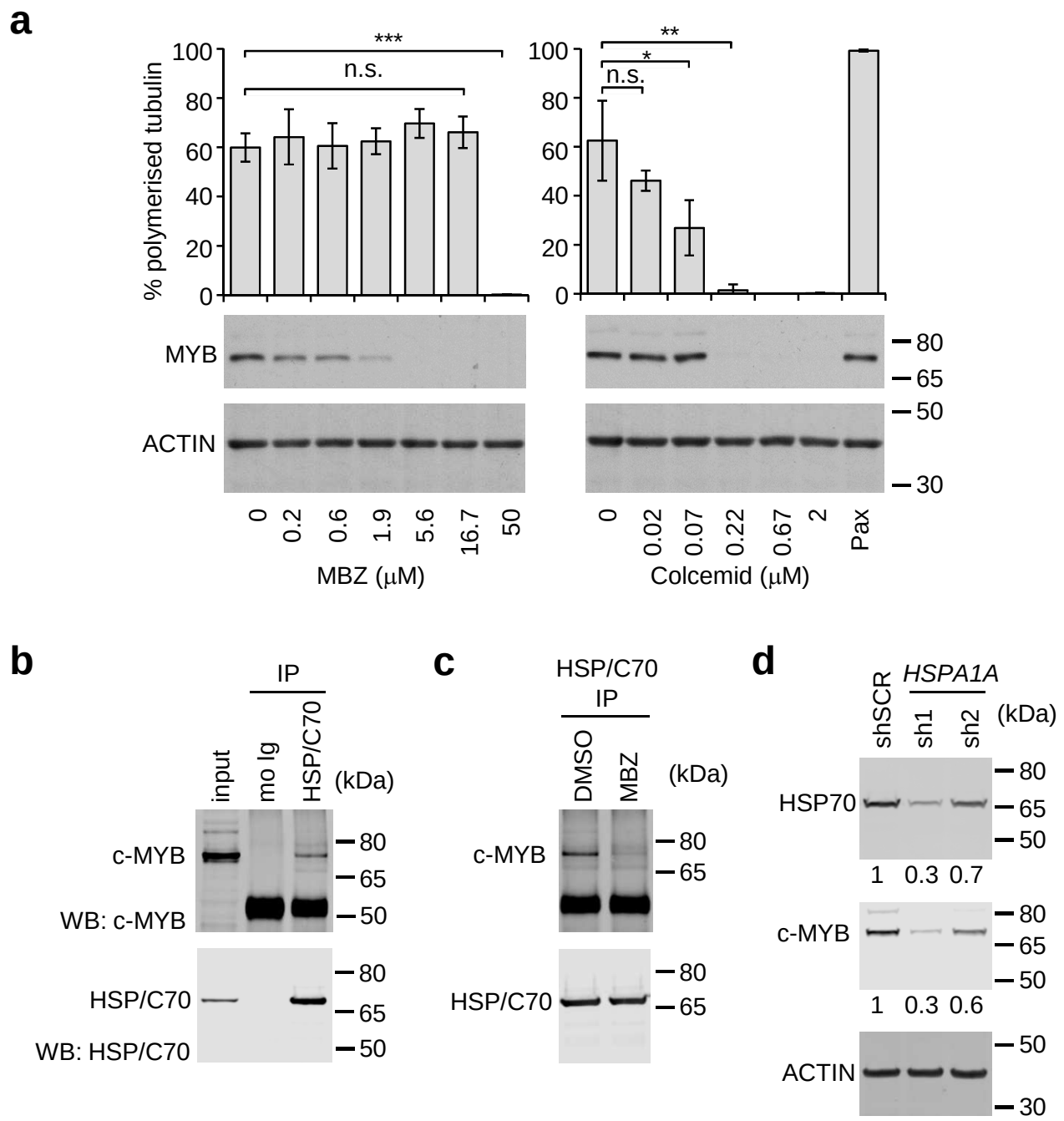
a
% polymerised tubulin
100
80
60
40
20
0
***
n.s.
**
*
n.s.
MYB
ACTIN
80
65
50
30
0
0.2
0.6
1.9
5.6
16.7
50
0
0.02
0.07
0.22
0.67
2
Pax
MBZ (μM)
Colcemid (μM)
b
IP
input
mo Ig
HSP/C70
(kDa)
c-MYB
WB: c-MYB
HSP/C70
WB: HSP/C70
c
HSP/C70
IP
DMSO
MBZ
(kDa)
c-MYB
HSP/C70
d
shSCR
HSPA1A
sh1
sh2
(kDa)
HSP70
1 0.3 0.7
c-MYB
1 0.3 0.6
ACTIN

FIGURE 4

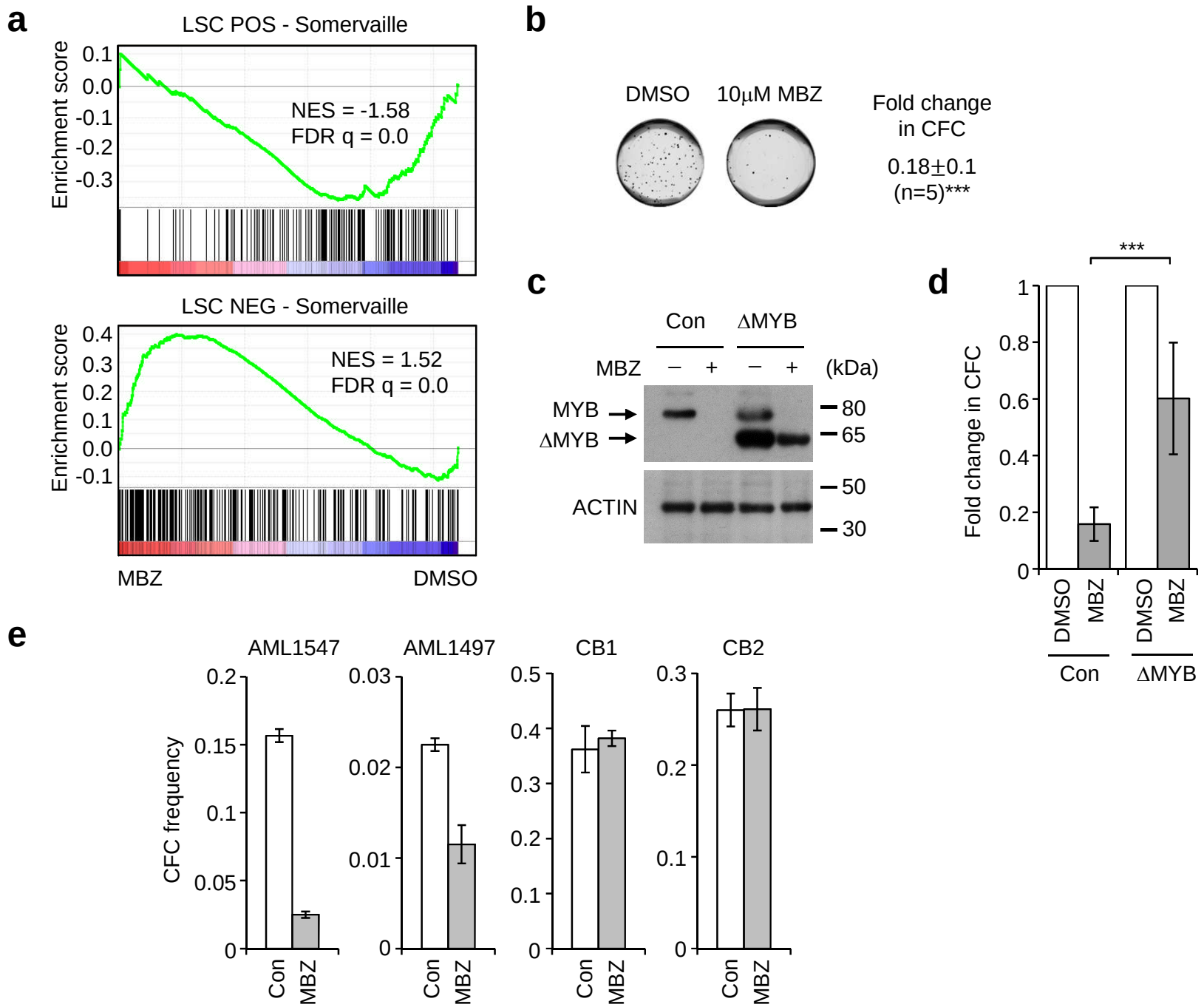
a
LSC POS - Somervaille
Enrichment score
0.1
0.0
-0.1
-0.2
-0.3
NES = -1.58
FDR q = 0.0
LSC NEG - Somervaille
Enrichment score
0.4
0.3
0.2
0.1
0.0
-0.1
NES = 1.52
FDR q = 0.0
MBZ
DMSO
b
DMSO
10μM MBZ
Fold change in CFC
0.18±0.1
(n=5)***
c
Con
ΔMYB
MBZ – + – +
(kDa)
MYB
ΔMYB
80
65
ACTIN
50
30
d
***
Fold change in CFC
1
0.8
0.6
0.4
0.2
0
DMSO
MBZ
DMSO
MBZ
Con
ΔMYB
e
AML1547
AML1497
CB1
CB2
CFC frequency
0.2
0.15
0.1
0.05
0
0.03
0.02
0.01
0
0.5
0.4
0.3
0.2
0.1
0
0.3
0.2
0.1
0
Con
MBZ

FIGURE 5

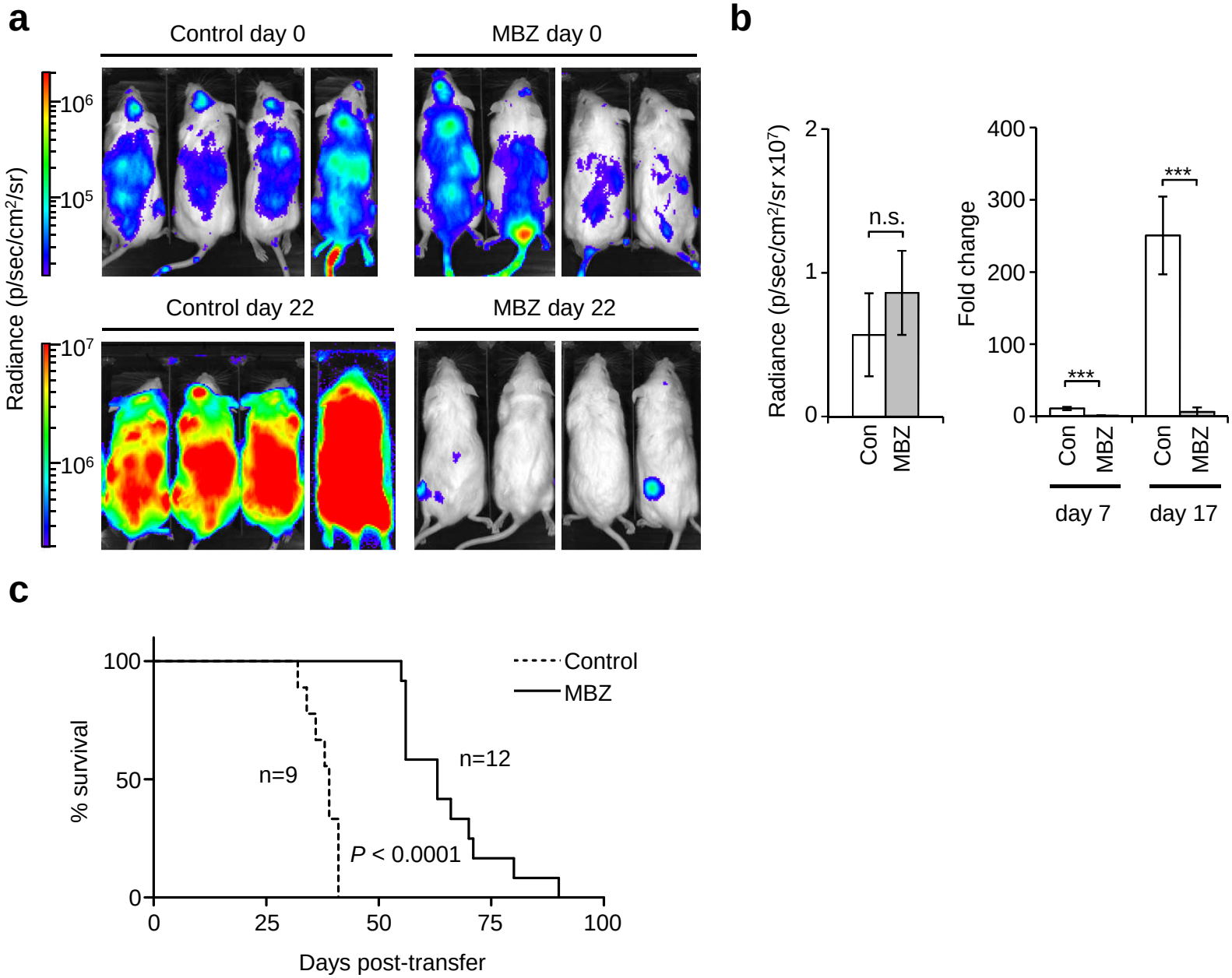
a
Control day 0
MBZ day 0
Control day 22
MBZ day 22
Radiance (p/sec/cm²/sr)
10⁶
10⁵
10⁷
10⁶
b
Radiance (p/sec/cm²/sr x10⁷)
2
1
0
n.s.
Con
MBZ
Fold change
400
300
200
100
0
***
***
Con
MBZ
Con
MBZ
day 7
day 17
c
% survival
100
50
0
Control
MBZ
n=9
n=12
P < 0.0001
0
25
50
75
100
Days post-transfer

FIGURE 6

SUPPLEMENTARY MATERIALS AND METHODS

Mice

All mice were maintained in the animal facilities of the UCL Great Ormond Street Institute of Child Health, London. All mouse experiments were performed according to and approved by the United Kingdom Home Office regulations and followed UCL Great Ormond Street Institute of Child Health institutional guidelines.

Human samples

Primary AML mononuclear cells were isolated by sucrose gradient centrifugation (Lymphoprep, 1.077 g/ml density; Nycomed Pharma).

Global gene expression analysis

Conditionally immortalized MLL-ENL and MLL-AF9 mouse myeloid cells have been previously described.[1-4] Control constitutive and conditionally immortalized cells were treated with 2 μg/ml doxycycline for 48 hours, RNA extracted using TRIzol reagent (ThermoFisher Scientific) and quality verified using an Agilent 2100 Bioanalyzer (Agilent Technologies, Wokingham, UK). RNA was hybridized to GeneChip Mouse Genome 430.2 arrays (Affymetrix). Data was analyzed using GeneSpring 7.3.1 software (Agilent Technologies). Gene expression changes of more than 2-fold, with a defined *P*-value cut-off ≤ 0.05, upon treatment with doxycycline were selected. Genes whose expression changed more than 2-fold in constitutive cells, upon doxycycline treatment, were excluded. Duplicate probe sets were removed, keeping those with the highest fold change. THP1 cells were cultured at 0.5×10^6 cells/ml and treated with 10 μM mebendazole or DMSO control, for 6 hours. RNA was purified and submitted to UCL Genomics for RNA-sequencing. Samples were processed using an Illumina TruSeq RNA sample prep kit Version 2 (RS-122-2001)

according to manufacturer's instructions (Illumina, Cambridge, UK) and sequenced on an Illumina NextSeq 500 (Illumina). Differential expression was obtained using the RNA Express BaseSpace® app (Illumina). Low expressed genes were removed from the output file. This was used for GSEA analysis.

Gene expression changes for SPIEDw analysis

MLL-ENL/MLL-AF9 gene expression changes, for genes also contained in the list of 1063 genes bound by c-MYB in mouse myeloid ERMYB cells[5] and deregulated in THP1 cells following siRNA-mediated c-MYB silencing,[6] were selected. These genes were converted into human gene names using the HGNC Comparison of Orthology Predictions (HCOP) search tool,[7] using the HGNC orthologs. This list (Supplementary Table 2) was then used to interrogate the CMAP database (https://portals.broadinstitute.org/cmap/)[8] using the SPIEDw web tool[9] (http://www.spied.org.uk/), which allows queries to be entered as gene names rather than probe sets.

Gene set enrichment analysis

c-MYB signatures[5] were genes bound by c-MYB in mouse myeloid ERMYB cells and deregulated in THP1 cells following siRNA-mediated c-MYB silencing,[6] either decreasing in expression (MYB activated) or increasing in expression more than 1.5-fold (MYB repressed). LSC signatures[10] consisted of probe sets positively correlated with LSC frequency (LSC POS) and negatively correlated with LSC frequency (LSC NEG). Mouse gene names were converted into human gene names using the HCOP using the HGNC orthologs, as above.

Cell culture and reagents

Human AML cell lines were cultured in RPMI or IMDM (SHI-1) supplemented with 10–20% FCS, L-glutamine and penicillin/streptomycin. 293FT (ThermoFisher Scientific) cells were maintained in DMEM with 10% FCS, L-glutamine, penicillin/streptomycin and 500 μg/ml G418. For some experiments, $CD34^+$ cord blood-derived cells (ZenBio) were expanded in StemSpan SFEM II medium (StemCell Technologies, Grenoble, France) supplemented with 100 ng/ml human SCF, TPO and FLT3L (all from Peprotech, London, UK).

Colony formation assays

AML cell lines were plated out in HSC002 methylcellulose medium (Bio Techne) at 150-500 cells/well in 24-well plates. Colonies were grown for 7-14 days and visualized by staining with 1 mg/ml p-iodonitrotetrazolium. For pre-stimulation, primary AML cells and normal $CD34^+$ cord blood-derived cells (ZenBio) were cultured with DMSO or 10 μM mebendazole for 20 hours in IMDM with 10% FCS, L-glutamine, penicillin/streptomycin. AML cells were supplemented with 100 ng/ml human SCF, TPO and FLT3L, 10 ng/ml IL3, IL6 and IL11, and $CD34^+$ cord blood-derived cells with 100 ng/ml human SCF, TPO and FLT3L (all growth factors were form Peprotech). Cells were plated out into HSC005 methylcellulose medium (Bio Techne) containing 50 ng/ml human SCF, 20 ng/ml IL3, IL6, G-CSFD, GM-CSF and 3 IU/ml EPO at 300-1000 cells/well in 35 mm plates. Primary AML methylcellulose cultures were further supplemented with 50 ng/ml TPO and FLT3L. Cultures were counted and morphology scored 14 days later.

Growth, apoptosis and cell cycle assays

The effect of mebendazole on growth of AML cell lines was examined by exposing them to different concentrations of mebendazole in liquid culture, starting at 1.25-2.5 x 10^5 cells/ml,

and 72 hours later were stained with TO-PRO®-3 (ThermoFisher Scientific) stain and total viable cells were determined by flow cytometry analysis on a BD FACSArray™ Bioanalyzer, using Summit 4.3 software (Beckman Coulter, High Wycombe, UK). Apoptosis was detected using the Annexin V Apoptosis detection kit (eBioscience, Hatfield, UK). Cell cycle analysis was performed using the Click-iT EdU Alexa Flour 647 Flow Cytometry Assay Kit (Invitrogen, Life Technologies). Cells were analyzed on an LSRII (BD Bioscience, San Jose, CA, USA), and the data were analyzed with Summit 4.3 software (Beckman Coulter).

Nematic protein organisation technique (NPOT) analysis

NPOT is a label free proprietary technology offered by INOVIEM Scientific, used to isolate and identify specific macromolecular scaffolds implemented in basic or pathological situations directly from human tissue. Specifically, primary AML sample AML4298 and THP1 cell homogenates were prepared under low temperature (4°C) in the absence of any detergent, reducing agent or protease or phosphatase inhibitors. All dilutions and washes were performed in HBSS with osmolality, trace elements, vitamins and salts concentrations as close as possible to those of the interstitial medium or cellular cytoplasm. Mebendazole (1µM) was added to the total tissue material. The macromolecular assemblies related to the specific ligands were then separated using a differential microdialysis system, based on liquid transitory pH gradient (pH5-10) where the macromolecules (protein groups) can migrate in the liquid phase to their mean molecular zwitterion positions.[11-14] The gradually growing and migrating macromolecules will form nematic crystals to macromolecular hetero-assemblies thanks to the molecular interactions between the ligand(s) and their targets. The hetero-assemblies are then trapped in mineral oil and isolated and identified by mass spectroscopy directly in liquid. Formation of hetero-assemblies and crystals were induced by addition of mebendazole and did not form in its absence.

In vivo transplantation

THP1 cells were transduced with a lentivirus vector containing a luciferase (LUC2)-IRES-EGFP cassette, and $EGFP^+$ cells purified by flow cytometric sorting. 1-2 x 10^6 THP1-LUC2 cells were transplanted into non-irradiated 6-12 week old male NOD-SCID-$\gamma^{-/-}$ (NSG; The Jackson Laboratory) mice by lateral tail vein injection. Recipient mice were imaged 10 minutes following subcutaneous injection of 5 mg/mouse D-luciferin (Cayman Chemical Company, Ann Arbor, MI, USA) using the IVIS® Lumina Series III pre-clinical *in vivo* imaging system (PerkinElmer) and randomly allocated to control or mebendazole-treated groups by flipping a coin. Mebendazole (200 mg/kg of diet) was administered *ad libitum* in regular powdered diet, changed daily. Group sizes were chosen based on previous estimates of disease latency in THP1 transplanted mice and experiments in the literature performing similar studies. No mice were excluded from the analysis. No blinding was used in group allocation or analysis of data.

Lentivirus vector cloning, production and transduction of cell lines

The ΔMYB cDNA[15] was cloned into the pCSGW-PIG vector, made by replacing the GFP cDNA from pCSGW[16] with a puro-IRES-GFP cassette, and the resulting vector used to transduce THP1 cells. The luciferase (LUC2) cDNA was cloned into pCSGW. Lentiviral MISSION shRNA constructs targeting c-MYB (Clone ID:NM_005375.2-927s21c1), HSPA1A (sh1:Clone ID:NM_005345.4-1539s1c1; sh2:Clone ID:NM_005345.4-566s1c1) and the scramble (SCR) non-silencing control (SHC002) were purchased from Sigma-Aldrich. The 293FT packaging cells (ThermoFisher Scientific) were transiently cotransfected with the lentiviral expression vectors, the pCMV-PAX2 construct and the pVSV-G envelope construct (kind gifts of D. Trono, Lausanne, Switzerland). Human leukemia cells were

transduced with lentiviral supernatant by spinoculation at 700g, 25°C for 45 minutes in the presence of 5 μg/mL polybrene. Transduced cells were selected in puromycin for 72 hours.

Western blot analysis

Cells were lysed in reducing sample buffer (100 mM dithiothreitol, 2% sodium dodecyl sulfate, 10 % glycerol, 0.002 % bromophenol blue, 62.5 mM Tris-HCL pH 6.8). Nuclear and cytoplasmic lysates were prepared using the Nuclear Extract kit (Active Motif, La Hulpe, Belgium). Protein samples were resolved on gels 10 % polyacrylamide (0.36 M bis-Tris, 10 % acrylamide/bis) in MOPS-SDS running buffer (50 mM Tris, 50 mM MOPS, 1 mM EDTA, 0.1 % SDS). Gels were transferred onto a PVDF (Merck Millipore) or nitrocellulose (LI-COR Biosciences, Cambridge, UK) membranes. Proteins were detected using appropriate secondary horseradish peroxidase-conjugated antibodies and visualized using a chemiluminescence reagent (GE Healthcare, Little Chalfont, UK) or IRDye 800CW and IRDye 680RD labelled secondary antibodies (LI-COR Biosciences). Quantification was performed on scanned unsaturated bands using the GS800 Imaging densitometer and Quantity One software (Bio-Rad Laboratories, Hemel Hempstead, UK) or on fluorescent images using the Odyssey® CLx and Image Studio software (LI-COR Biosciences).

Microtubule depolymerization assay

AML cells were treated for 6 hours with mebendazole, colcemid (ThermoFisher Scientific) or paclitaxel (Cayman Chemical Company). 1 x 10^6 cells were washed twice in PBS and resuspended in 100 μl depolymerization buffer (20mM Tris-HCl pH6.8, 0.14 M NaCl, 0.5% NP-40, 1 mM $MgCl_2$, 2 mM EGTA, 10 μM paclitaxel, protease inhibitors)[17] and vortexed on maximum setting. Lysis of cells with this microtubule-stabilizing buffer preserves the proportions of polymerized and soluble microtubules present *in vivo* in cells, following the

period of drug treatment. Cells were then centrifuged at 12,000 x g for 10 min at 4^0C. The supernatant was decanted and 100 μl 2x reducing sample buffer added (S, soluble tubulin). The pellet was resuspended in 100 μl 1 mM $CaCl_2$ (with protease inhibitors), incubated at room temperature for 15 minutes, with brief vortexing and 100 μl 2x reducing sample buffer added (P, lysate pellet). Percent polymerized tubulin was calculated from the formula P/(P + S)100 from quantified western blot bands.

Quantitative RT-PCR analysis

Total RNA was isolated from cells using RNeasy Mini Kit (Qiagen, Manchester, UK) according to the manufacturer's instructions. RNA was converted into cDNA using a cDNA synthesis kit (Invitrogen, Life Technologies) according to the manufacturer's instructions. Samples were treated with DNase I (Invitrogen, Life Technologies) prior to reverse transcription using the Moloney murine leukemia virus reverse transcriptase (Invitrogen, Life Technologies).

SUPPLEMENTARY REFERENCES

1 Horton SJ, Grier DG, McGonigle GJ, Thompson A, Morrow M, De Silva I, *et al.* Continuous MLL-ENL expression is necessary to establish a "Hox Code" and maintain immortalization of hematopoietic progenitor cells. *Cancer Res* 2005; 65: 9245-9252.

2 Horton SJ, Walf-Vorderwulbecke V, Chatters SJ, Sebire NJ, de Boer J, Williams O. Acute myeloid leukemia induced by MLL-ENL is cured by oncogene ablation despite acquisition of complex genetic abnormalities. *Blood* 2009; 113: 4922-4929.

3 Walf-Vorderwulbecke V, de Boer J, Horton SJ, van Amerongen R, Proost N, Berns A, *et al.* Frat2 mediates the oncogenic activation of Rac by MLL fusions. *Blood* 2012; 120: 4819-4828.

4 Osaki H, Walf-Vorderwulbecke V, Mangolini M, Zhao L, Horton SJ, Morrone G, *et al.* The AAA+ ATPase RUVBL2 is a critical mediator of MLL-AF9 oncogenesis. *Leukemia* 2013; 27: 1461-1468.

5 Zhao L, Glazov EA, Pattabiraman DR, Al-Owaidi F, Zhang P, Brown MA, *et al.* Integrated genome-wide chromatin occupancy and expression analyses identify key myeloid pro-differentiation transcription factors repressed by Myb. *Nucleic Acids Res* 2011; 39: 4664-4679.

6 Suzuki H, Forrest AR, van Nimwegen E, Daub CO, Balwierz PJ, Irvine KM, *et al.* The transcriptional network that controls growth arrest and differentiation in a human myeloid leukemia cell line. *Nat Genet* 2009; 41: 553-562.

7 Eyre TA, Wright MW, Lush MJ, Bruford EA. HCOP: a searchable database of human orthology predictions. *Brief Bioinform* 2007; 8: 2-5.

8 Lamb J, Crawford ED, Peck D, Modell JW, Blat IC, Wrobel MJ, *et al.* The Connectivity Map: using gene-expression signatures to connect small molecules, genes, and disease. *Science* 2006; 313: 1929-1935.

9 Williams G. SPIEDw: a searchable platform-independent expression database web tool. *BMC Genomics* 2013; 14: 765.

10 Somervaille TC, Matheny CJ, Spencer GJ, Iwasaki M, Rinn JL, Witten DM, *et al.* Hierarchical maintenance of MLL myeloid leukemia stem cells employs a transcriptional program shared with embryonic rather than adult stem cells. *Cell Stem Cell* 2009; 4: 129-140.

11 Bolen DW, Baskakov IV. The osmophobic effect: natural selection of a thermodynamic force in protein folding. *J Mol Biol* 2001; 310: 955-963.

12 Shimizu S. Estimating hydration changes upon biomolecular reactions from osmotic stress, high pressure, and preferential hydration experiments. *Proc Natl Acad Sci U S A* 2004; 101: 1195-1199.

13 Zhou HX, Rivas G, Minton AP. Macromolecular crowding and confinement: biochemical, biophysical, and potential physiological consequences. *Annu Rev Biophys* 2008; 37: 375-397.

14 Gee MB, Smith PE. Kirkwood-Buff theory of molecular and protein association, aggregation, and cellular crowding. *J Chem Phys* 2009; 131: 165101.

15 Corradini F, Cesi V, Bartella V, Pani E, Bussolari R, Candini O, *et al.* Enhanced proliferative potential of hematopoietic cells expressing degradation-resistant c-Myb mutants. *J Biol Chem* 2005; 280: 30254-30262.

16 Demaison C, Parsley K, Brouns G, Scherr M, Battmer K, Kinnon C, *et al.* High-level transduction and gene expression in hematopoietic repopulating cells using a human immunodeficiency [correction of imunodeficiency] virus type 1-based lentiviral vector containing an internal spleen focus forming virus promoter. *Hum Gene Ther* 2002; 13: 803-813.

17 Minotti AM, Barlow SB, Cabral F. Resistance to antimitotic drugs in Chinese hamster ovary cells correlates with changes in the level of polymerized tubulin. *J Biol Chem* 1991; 266: 3987-3994.

Supplementary Figure Legends

Supplementary Figure 1. Mebendazole inhibits expression of c-MYB targets in AML cells. QPCR analysis of selected c-MYB target gene expression in THP1 cells after 6 hours treatment with DMSO or 10 μM mebendazole, normalized to DMSO controls. Bars and error bars are means and SD of three independent experiments. $^{**}P < 0.01$; $^{***}P < 0.001$; $^{****}P < 0.0001$; n.s. not significant (relative to DMSO controls), one sample *t* test.

Supplementary Figure 2. Mebendazole inhibits growth and induces apoptosis in AML cells. (**a**) The chart shows the fold change in viable cell number of AML cell lines treated with DMSO or 10 μM mebendazole, over 72 hours. Symbols and error bars are means and SD of three independent experiments, each in triplicate. (**b**) Examples of Annexin V/PI staining of THP1 cells exposed to DMSO or 10μM mebendazole for 48 hours. (**c**) Apoptotic analysis of AML cell lines exposed to DMSO or 10 μM mebendazole, over 72 hours. Symbols, representing the percentage of Annexin V^-/PI^- cells, and error bars are means and SD of three independent experiments.

Supplementary Figure 3. Mebendazole inhibits colony formation by AML cells. Colony formation, normalized to DMSO controls, of AML cell lines in the presence of indicated mebendazole concentrations. Bars and error bars are means and SD of three independent experiments, each in quadruplicate.

Supplementary Figure 4. *c-MYB* silencing inhibits colony formation by AML cells. (**a**) Western blot analysis of c-MYB protein expression in AML cells transduced with control scramble (SCR) shRNA or shRNA targeting c-MYB (MYB). (**b**) Example of colony formation in methylcellulose cultures of shSCR or shMYB transduced THP1 cells. (**c**) Colony formation, normalized to DMSO controls, of shSCR or shMYB transduced AML cell lines. Bars and error bars are means and SD of quadruplicate cultures.

Supplementary Figure 5. Proteasomal inhibition blocks mebendazole induced c-MYB degradation. Quantification of c-MYB protein expression in indicated AML cells lines following 6 hours treatment with DMSO, 10 μM MBZ or 10 μM MBZ/10 μM MG132. Bars and error bars are means and SD of four (THP1) and three (OCI-AML3, SHI-1) independent experiments. Data are normalized to DMSO controls. ***$P < 0.001$; n.s. not significant (relative to DMSO controls), one sample *t* test.

Supplementary Figure 6. Mebendazole induces c-MYB degradation at lower concentrations than those required for tubulin depolymerization. (**a**) Example of western blot analysis of tubulin depolymerization assay. Polymerized tubulin, present in the lysate pellet (P), and soluble tubulin (S) bands are shown for THP1 cells treated for 6 hours with indicated concentrations of mebendazole (top) or colcemid and 5 μM paclitaxel (Pax) (bottom). (**b**) Percent polymerized tubulin in OCI-AML3 cells following 6 hours treatment with indicated concentrations of mebendazole (top left) or colcemid (top right), and western blot analysis of corresponding c-MYB protein expression (bottom). Tubulin stabilization by 5 μM paclitaxel (Pax) is also shown. Bars and error bars are means and SD, respectively, of four independent experiments. *$P < 0.05$; ***$P < 0.001$, n.s. not significant, unpaired Student's t-test.

Supplementary Figure 7. Mebendazole induced c-MYB loss is not due to cell cycle inhibition. (**a**) Quantification of c-MYB protein expression in THP1 cells following 4 hours treatment with DMSO or indicated concentrations of mebendazole. Bars and error bars are means and SD of four independent experiments. Data are normalized to DMSO controls. (**b**) Apoptotic analysis of THP1 cells following 4 hours exposure to DMSO or 10 μM mebendazole. Bars, representing the percentage of Annexin V^-/PI^- cells, and error bars are means and SD of three independent experiments. (**c**) Examples of flow cell cycle cytometry plots of THP1 cells treated for 4 hours with DMSO or the indicated concentrations of

mebendazole. Numbers inside plots are percentages of cells in Go/G1 (bottom left), S (top) and G2/M (bottom right) phases of the cell cycle. (**d** and **e**) Bars and error bars are means and SD of percentages of THP1 cells in the Go/G1, S and G2/M phases of the cell cycle following 4 (**d**) and 24 (**e**) hours of treatment with DMSO or the indicated concentrations of mebendazole, from four (**d**) and three (**e**) independent experiments. ***$P < 0.001$; n.s. not significant, unpaired Student's t-test.

Supplementary Figure 8. Nematic protein organisation technique (NPOT) analysis of mebendazole in AML cell lysates. (**a**) Pictures of three independent hetero-assemblies (circled in red) induced by mebendazole in primary AML sample AML4298 and THP1 cell lysates. (**b**) Venn diagrams for the number of proteins identified in AML4298 and THP1 lysates, and in both lysates. (**c**) DAVID analysis and the annotation sources GOTERM_BP2 (Biological process) were used to identify the functional categories identified in AML4298 lysates. Shown in bold are the proteins comprising the 'protein folding' category also identified in THP1 lysates.

Supplementary Figure 9. The HSP70/HSC70 chaperone complex binds c-MYB and is required for maintenance of c-MYB protein expression. (**a**) Western blot analysis of mouse IgG and anti-c-MYB immunoprecipitates from THP1 cells, stained with anti-HSP70/HSC70 (top) and anti-c-MYB (bottom). Representative data from one of three independent experiments. (**b**) Quantification of HSP70 (left) and c-MYB (right) protein expression in THP1 cells 7 days after transduction with control scramble (shSCR) shRNA or two independent shRNA targeting *HSPA1A* (sh1 and sh2). Bars and error bars are means and SD of three independent experiments. (**c**) Representative data and quantification of c-MYB protein expression in THP-1 cells after 6 hours treatment with DMSO or the indicated concentrations of the HSP70 inhibitors, KNK437 and VER-155008. Bars and error bars are means and SD of three independent experiments. (**d**) Representative data and quantification

of HSP70/HSC70 protein expression in total (total), cytoplasmic (cyto) and nuclear (nuc) extracts from THP-1 cells treated with DMSO or 10 μM mebendazole for 6 hours. The extracts were validated using antibodies against αTubulin (cytoplasmic) and SP1 (nuclear), and nuclear expression of c-MYB is also shown. Bars and error bars represent relative HSP70/HSC70 expression in total (using αTubulin for loading), cytoplasmic (using αTubulin for loading) and nuclear extracts (using SP1 for loading), and are means and SD of three independent experiments. *$P < 0.05$; **$P < 0.01$; ***$P < 0.001$; n.s. not significant (relative to DMSO controls), one sample *t* test.

Supplementary Figure 10. Mebendazole pre-treatment inhibits colony formation by primary AML cells but not $CD34^+$ CB cells. (**a**) Example of colony formation by a primary AML patient sample (AML1547) and a normal $CD34^+$ cord blood sample (CB1), after pre-treatment with DMSO or 10 μM mebendazole. Cells were treated with vehicle or drug for 20 hours, washed and placed into methylcellulose culture. Colonies were grown for 14 days and visualized by staining with 1 mg/ml p-iodonitrotetrazolium. (**b**) CFU-G, CFU-GM, BFU-E, CFU-M, CFU-GEMM and total colony numbers of two independent normal $CD34^+$ cord blood samples (CB1, CB2) after pre-treatment with DMSO or 10 μM mebendazole. Cells were treated with vehicle or drug for 20 hours, washed and placed into methylcellulose culture, and colony formation scored 14 days later.

Supplementary Figure 11. Mebendazole induced c-MYB loss in CB cells is less acute than in AML cells. (**a**) Representative data and (**b**) quantification of c-MYB protein expression in CB cells following treatment with DMSO or 10 μM mebendazole for 6 hours. Prior to drug treatment, $CD34^+$ CB cells were expanded for 7 days. Bars and error bars are means and SD of data from three independent CB samples. *$P < 0.05$ (relative to DMSO controls), one sample *t* test.

Supplementary Figure 12. *In vivo* drug treatment selects for increased c-MYB expression and reduced sensitivity to mebendazole. (**a**) Quantification of c-MYB protein expression in THP1 cells *ex vivo* (T-RES1), isolated from NSG mice following treatment with mebendazole *in vivo*, compared to control THP1 cells. (**b**) Increased c-MYB expression is still exhibited after two weeks *in vitro* culture in the absence of mebendazole. c-MYB protein expression in THP1 cells isolated from mebendazole-treated NSG mice (T-RES1 and T-RES2) following 2 weeks *in vitro* culture (*in vitro*). (**c**) c-MYB protein expression in T-RES1 cells, after 6 hours *ex vivo* exposure to the indicated concentrations of mebendazole, compared to control THP1 cells. (**d**) Viability, normalized to DMSO controls, of control THP1 and T-RES1 cells treated for 72 hours with indicated mebendazole concentrations. Bars and error bars are means and SD of triplicate cultures.

Supplementary Table 1. Patient characteristics.

Patient id	Sex	Age (yrs)	FAB	Karyotype
1497	M	1.6	4	46, XY, t(9;11;9)(p22;p23;q34)
1547	F	8.8	5	46, XX, t(9;11)(p22;q23)(low% 47, idem, +8)
4298	M	11.2	5	46, XY, t(9;11)

Supplementary Table 2. Gene expression data for SPIEDw analysis.

Gene	Fold change upon loss of MLL-ENL/MLL-AF9
ANTXR1	-14.040
SIX4	-9.696
P2RY2	-7.474
FRAT2	-6.627
IRAK1BP1	-5.853
IPO11	-5.278
LRIG1	-4.860
SIX1	-3.968
TASP1	-3.809
CABLES1	-3.734
MYC	-3.724
MMACHC	-3.586
PDCD4	-3.571
NT5DC2	-3.562
PDXK	-3.490
ST7	-3.435
MID1	-3.373
SPRED1	-3.043
PFKL	-3.026
HSPA2	-2.994
MRPS27	-2.957
PRMT6	-2.933
SLC39A8	-2.867
MRPS6	-2.862
MSI2	-2.786
GATA2	-2.744
UCK2	-2.714
STEAP3	-2.714
PRPF19	-2.664
CRTAP	-2.642
EXOSC6	-2.631
GPR180	-2.629
LIPT1	-2.617
PAPSS2	-2.613
AHCY	-2.607
EBNA1BP2	-2.563
TMEM97	-2.558
ABI2	-2.554
BAMBI	-2.548
PCDH7	-2.547
TRAP1	-2.518
MINPP1	-2.490
PRPS1	-2.452

SPRED2	-2.409
POLR1E	-2.275
SPRY2	-2.226
OLA1	-2.198
LIMK1	-2.182
COMMD9	-2.172
NUP35	-2.151
ACSL3	-2.149
KLHL5	-2.147
LPAR1	-2.132
DTYMK	-2.103
EPRS	-2.099
IDH2	-2.095
TMEM107	-2.080
TRIM45	-2.057
SASH1	-2.045
CXorf21	-2.029
BCLAF1	-2.005
NIT2	-1.992
SNRPF	-1.988
IL13RA1	1.992
ECM1	2.004
AGTRAP	2.004
RUNX1	2.020
CENPJ	2.024
PSAP	2.037
PTPRC	2.041
DACH1	2.053
FMNL1	2.053
SULF2	2.058
SLA	2.070
SSH1	2.070
PTK2B	2.070
ABCG1	2.088
PLEK	2.092
INTS12	2.096
TDRD7	2.119
PLEKHO2	2.123
CDC42EP3	2.132
RBMS1	2.132
IQSEC1	2.132
FHOD1	2.141
LST1	2.146
H2AFX	2.151
NUMB	2.160
ACVR1B	2.165
ABCA13	2.165
IQGAP1	2.174

TOB1	2.174
WDR26	2.174
PLEKHA2	2.179
DMXL2	2.217
AKAP13	2.222
MAPK3	2.227
PRKCD	2.252
IFT122	2.257
PIK3CB	2.262
HBP1	2.304
SSH2	2.309
PTPRE	2.326
LPP	2.342
SH3KBP1	2.347
PYGL	2.347
MBP	2.381
WIPI1	2.381
HEXB	2.410
RTKN2	2.427
TNFAIP3	2.451
PHF21A	2.457
KLF13	2.457
GLRX	2.481
FLNA	2.488
NCF4	2.494
PSTPIP2	2.513
FLOT1	2.525
SMARCA2	2.538
NEU1	2.558
SNX10	2.558
RAC2	2.591
SIRPA	2.660
VCAN	2.667
SEMA4D	2.695
ITGAL	2.710
JAZF1	2.747
KLF6	2.762
IQGAP2	2.778
BMX	2.786
MYO1F	2.874
SORL1	2.882
LTA4H	2.890
PELI2	2.907
ACSL1	2.933
MYH9	2.933
SPSB1	2.976
SNAI3	3.012
CD9	3.012

RHBDF2	3.030
CCND3	3.040
THBS1	3.077
DOCK5	3.125
LGALS3	3.226
PLAUR	3.268
ZFP36	3.390
ZYX	3.390
ZFP36L1	3.509
GLIPR2	3.636
DHRS3	3.650
NOTCH1	3.676
ST3GAL2	3.690
NFKBIZ	3.831
PLAU	3.906
LTB4R	3.922
NCF1	4.000
FGR	4.219
LYST	4.237
DAPK2	4.274
PHLDA1	4.367
BCL6	4.425
SQRDL	4.785
GPAT3	5.181
GCNT2	5.435
HLX	6.024
SERPINB2	6.452
S100A4	8.130
EGR2	9.259
CAMP	9.434
PLP2	9.615
HCK	9.709
PRAM1	12.422
C5AR1	13.889

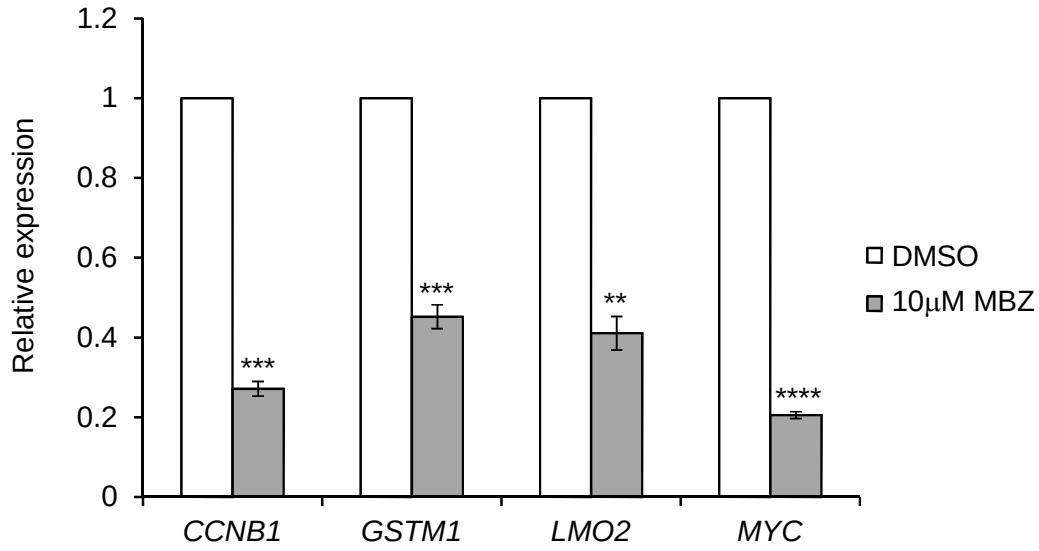

SUPPLEMENTARY FIGURE 1

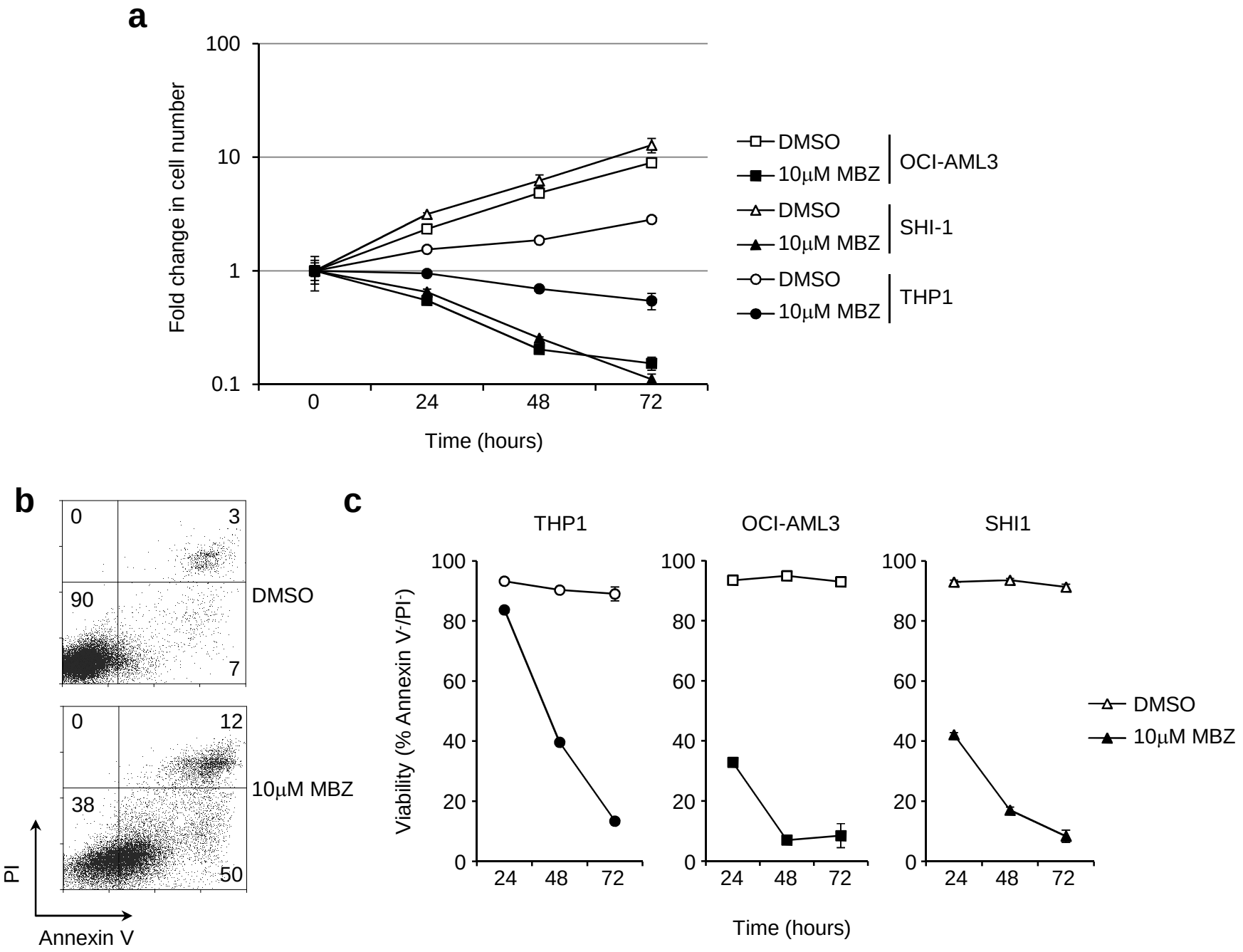

SUPPLEMENTARY FIGURE 2

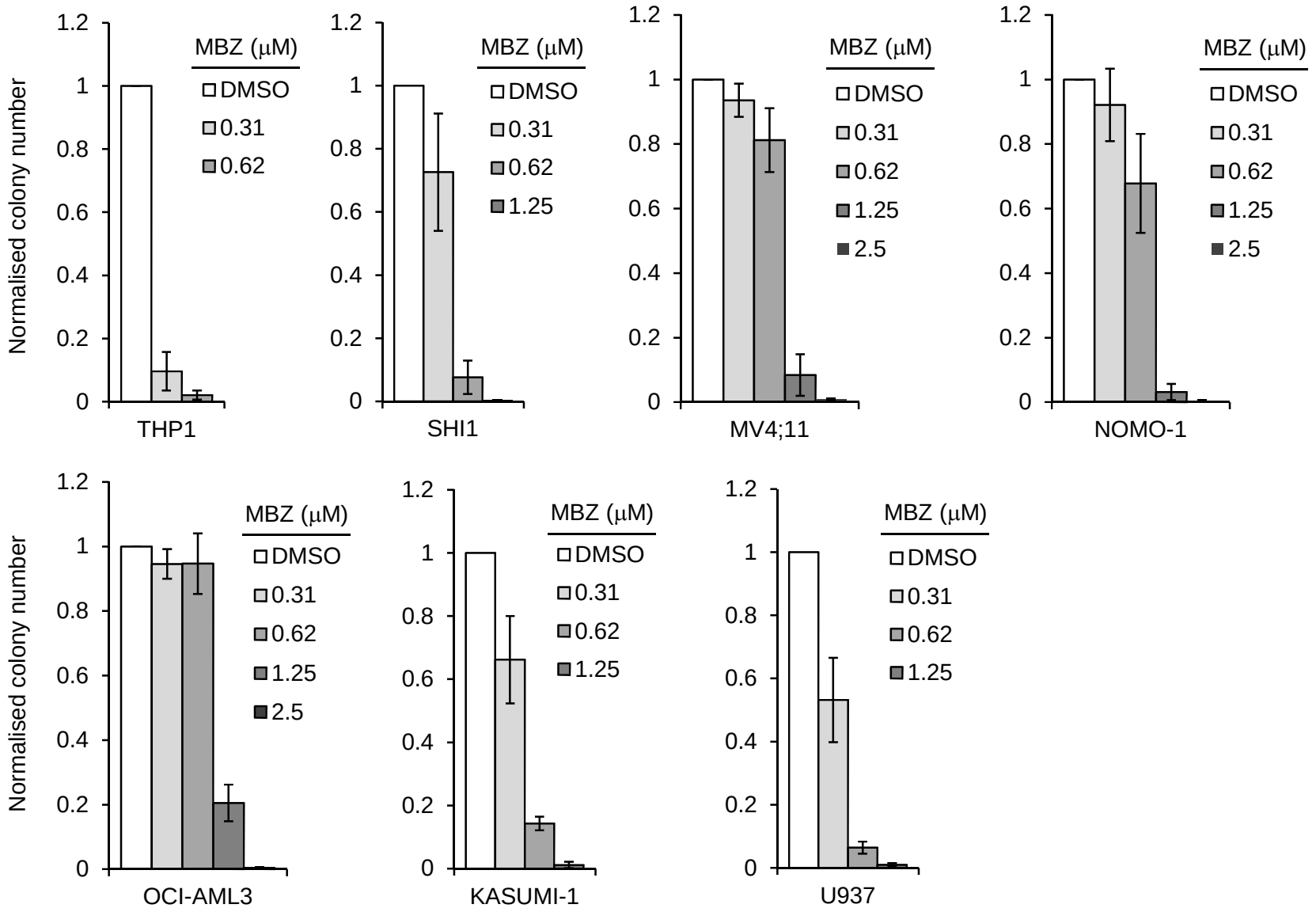

SUPPLEMENTARY FIGURE 3

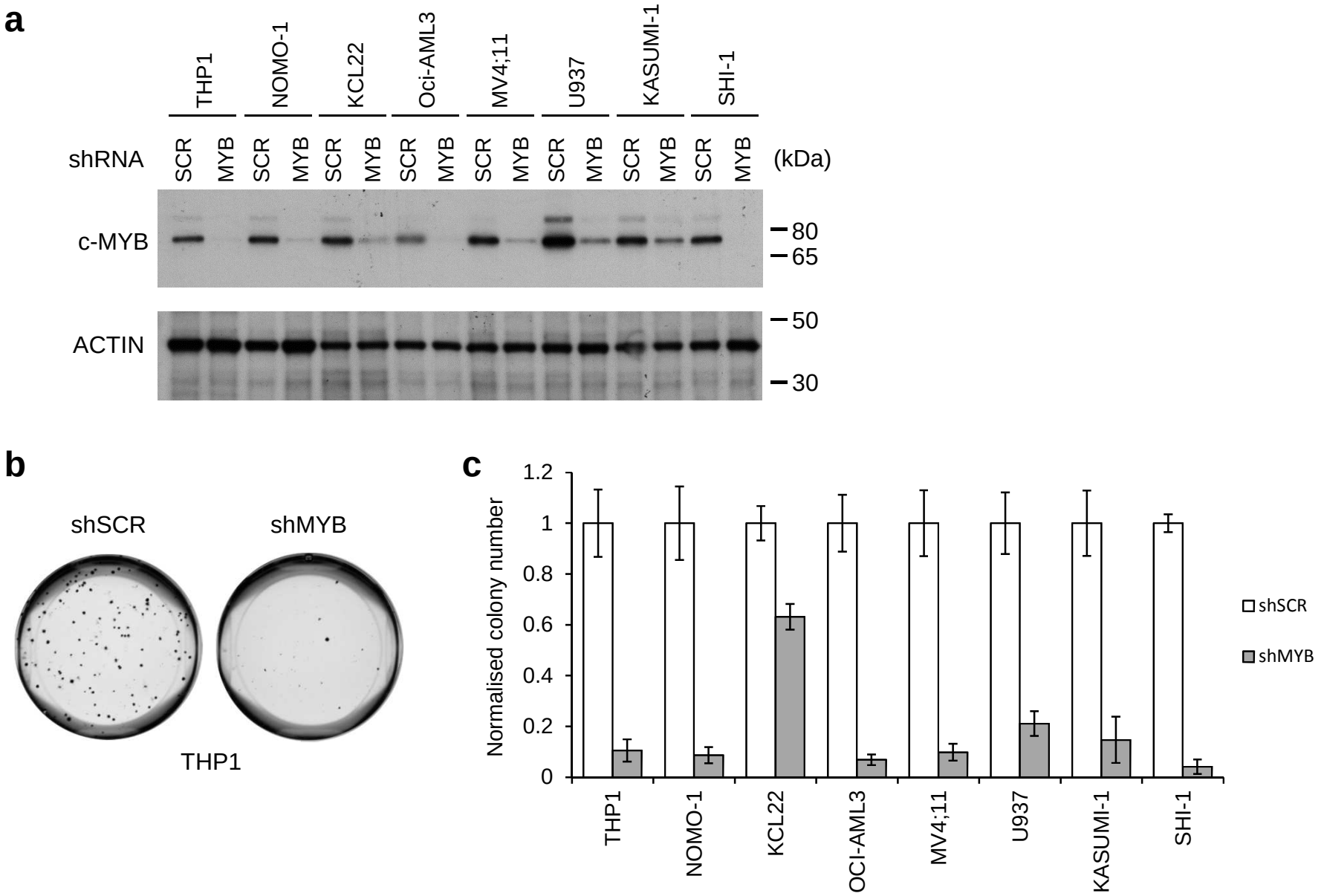

SUPPLEMENTARY FIGURE 4

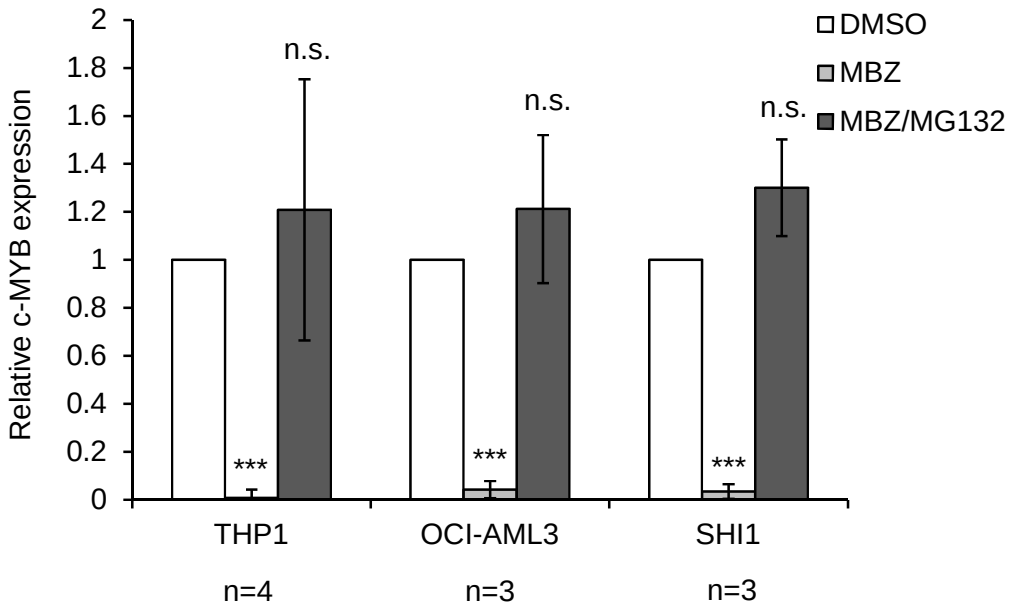

SUPPLEMENTARY FIGURE 5

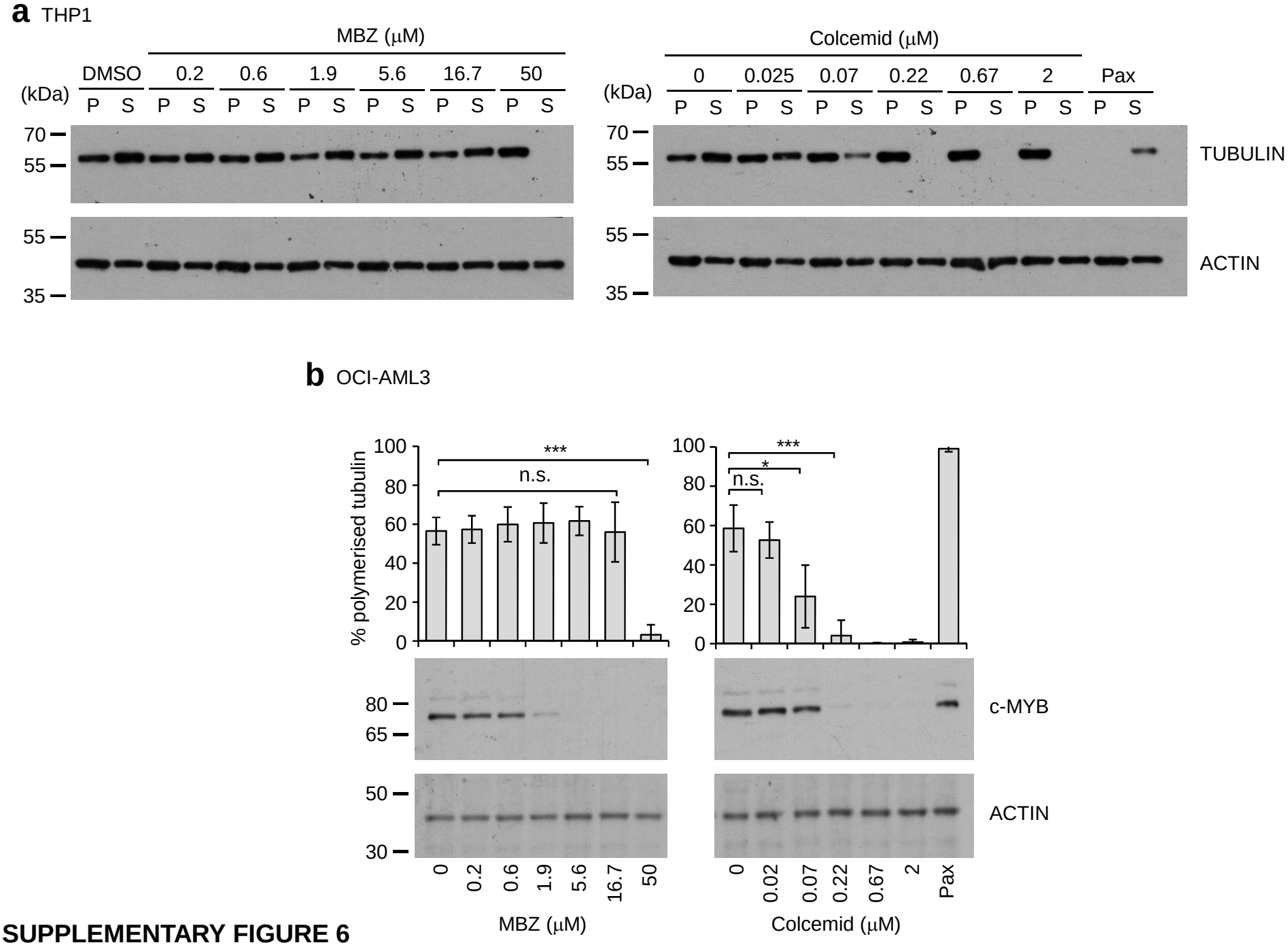

SUPPLEMENTARY FIGURE 6

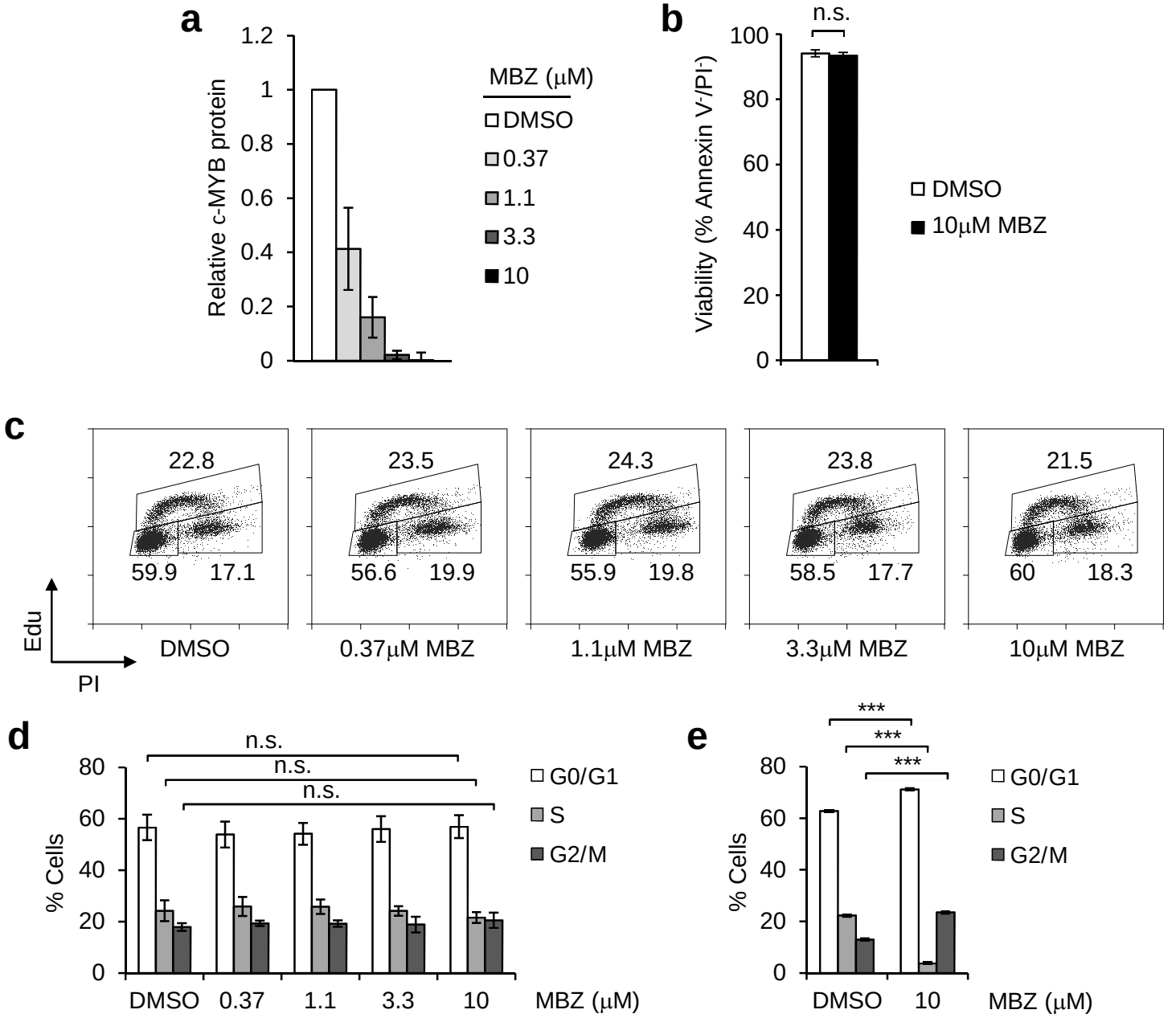

SUPPLEMENTARY FIGURE 7

a

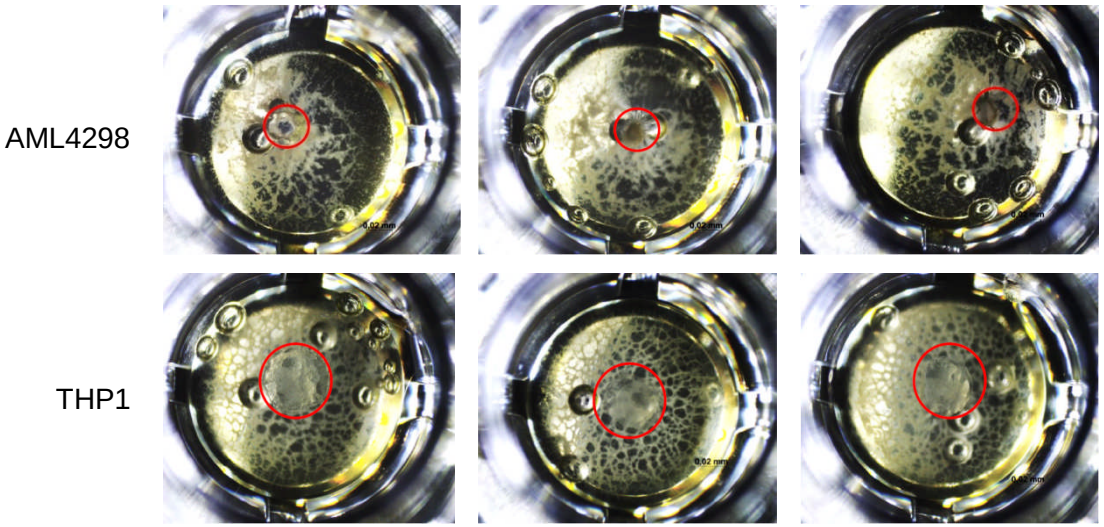

b

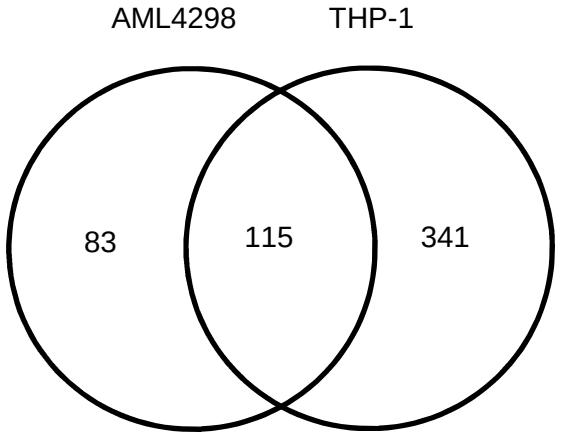

c

David analysis patient sample AML4298 with MBZ

Category	No of Proteins	P value
single-organism metabolic process	86	8.00E-10
protein folding	16	6.20E-08
cell adhesion	44	4.40E-07
catabolic process	48	1.10E-06
cellular component biogenesis	59	8.10E-06

alanyl-tRNA synthetase(AARS)
glucosidase II alpha subunit(GANAB)
heat shock protein 90 alpha family class A member 1(HSP90AA1)
heat shock protein 90 alpha family class B member 1(HSP90AB1)
heat shock protein family A (Hsp70) member 1A(HSPA1A)
heat shock protein family A (Hsp70) member 6(HSPA6)
heat shock protein family A (Hsp70) member 8(HSPA8)
heat shock protein family A (Hsp70) member 9(HSPA9)
heat shock protein family D (Hsp60) member 1(HSPD1)
peptidylprolyl isomerase A(PPIA)
peptidylprolyl isomerase B(PPIB)
protein disulfide isomerase family A member 3(PDIA3)
protein disulfide isomerase family A member 6(PDIA6)
protein kinase C substrate 80K-H(PRKCSH)
RuvB like AAA ATPase 2(RUVBL2)
TNF receptor associated protein 1(TRAP1)

*In bold confirmed in THP-1 cells.

SUPPLEMENTARY FIGURE 8

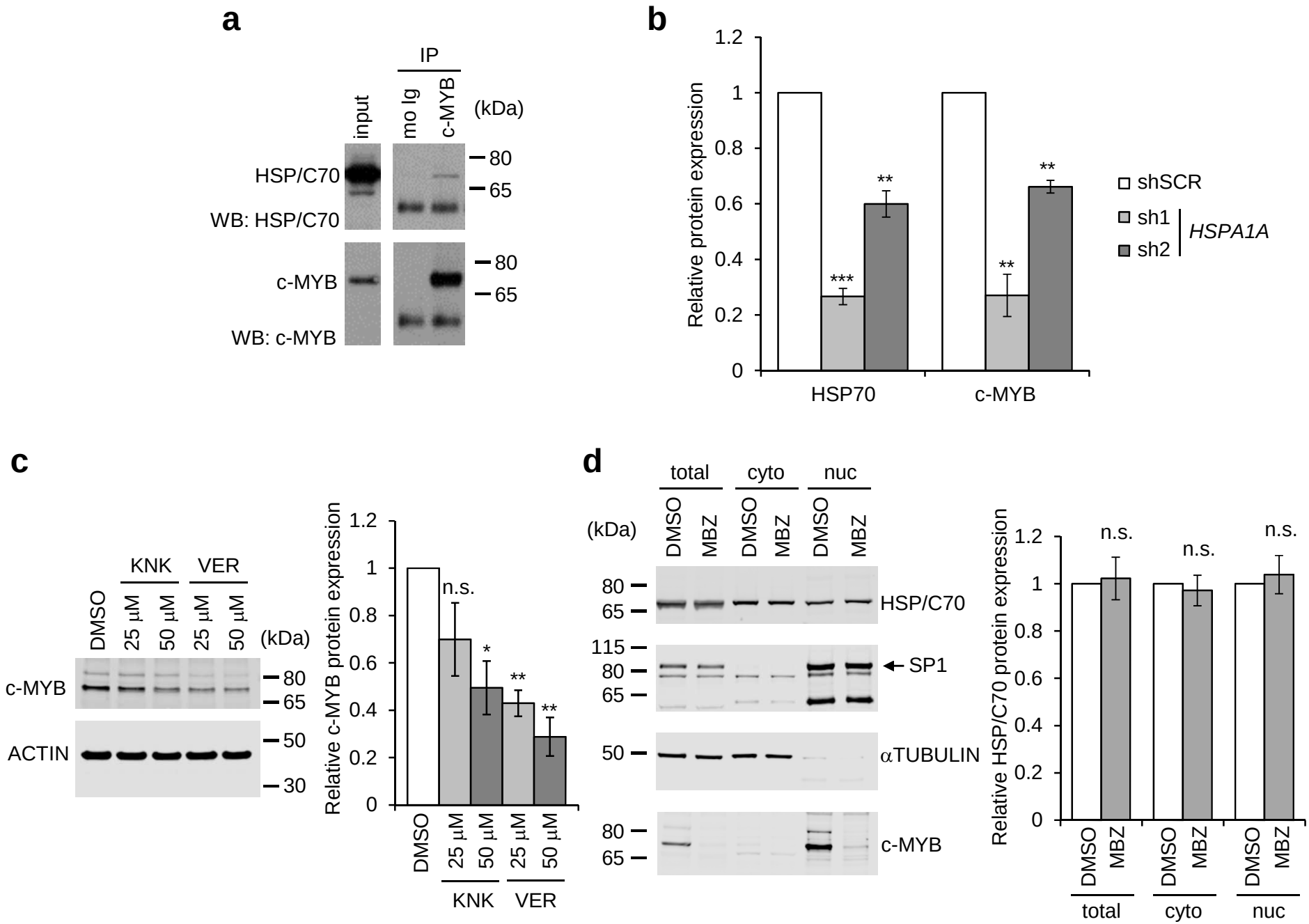

SUPPLEMENTARY FIGURE 9

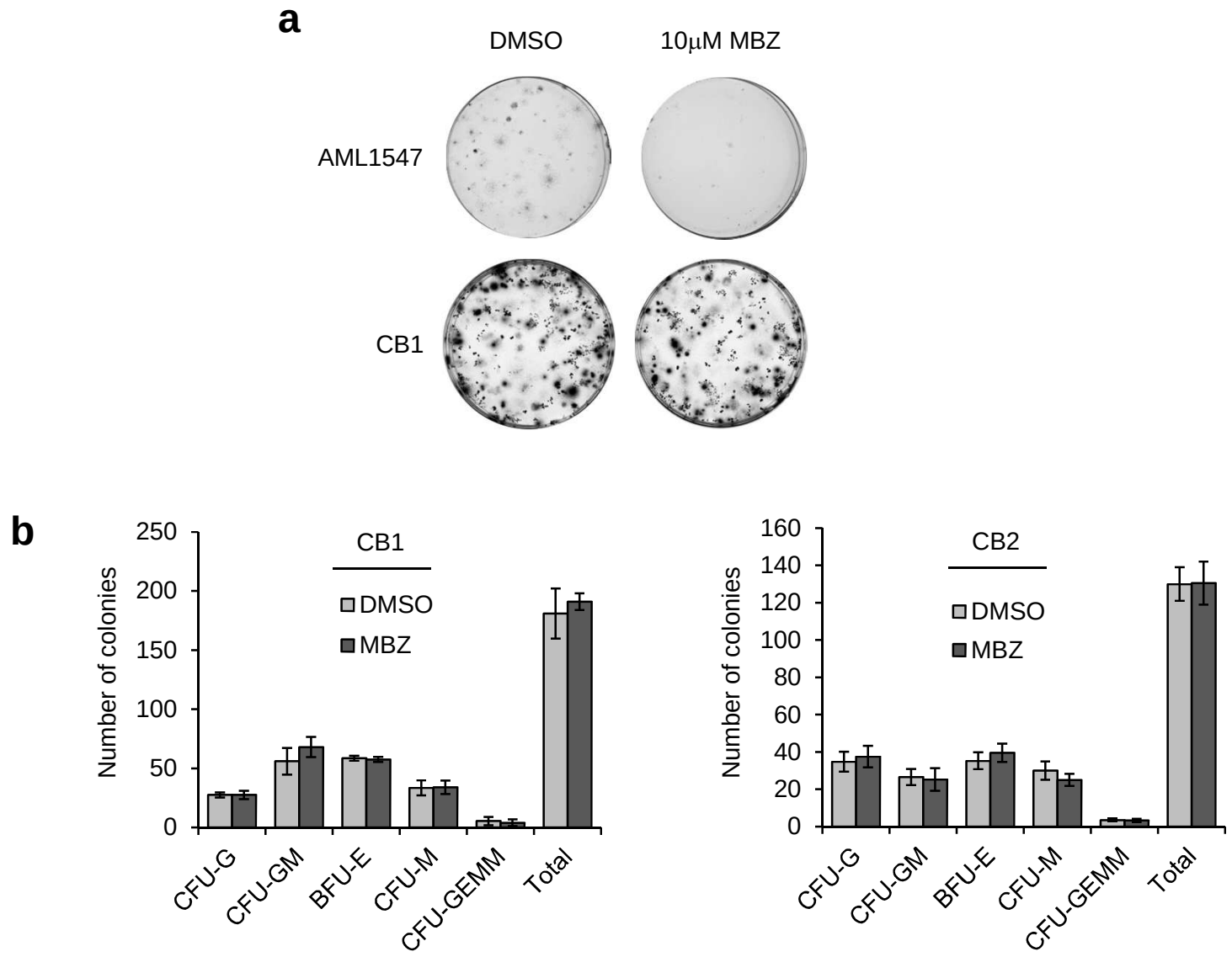

SUPPLEMENTARY FIGURE 10

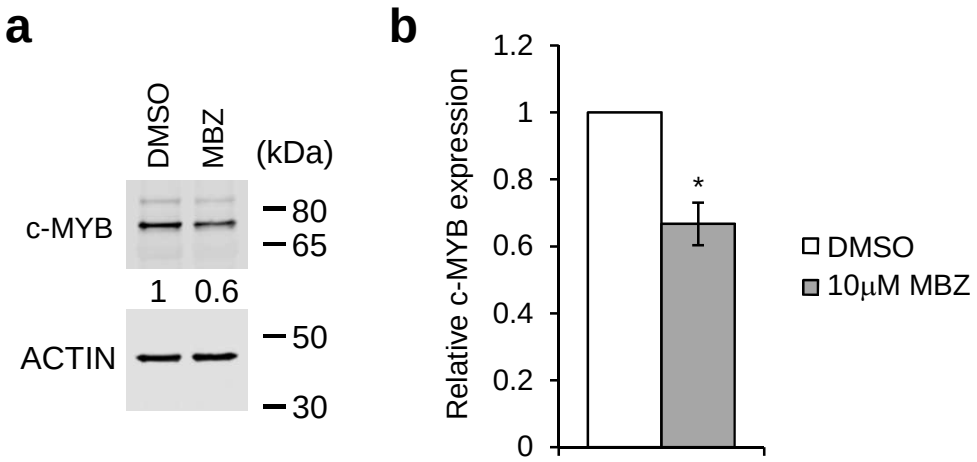

SUPPLEMENTARY FIGURE 11

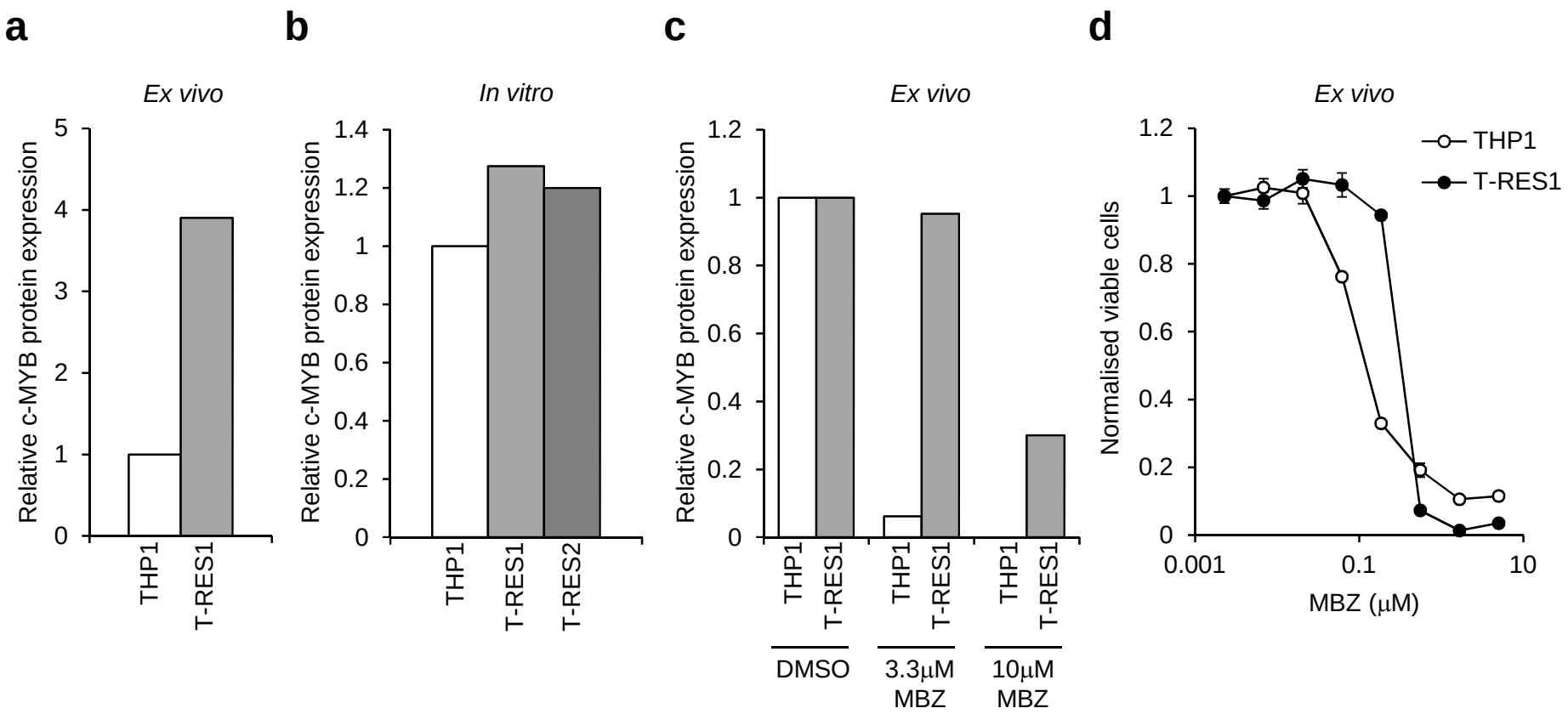

SUPPLEMENTARY FIGURE 12